Inorganic Chemistry

Article

pubs.acs.org/IC

Influence of the Solvent and Metal Center on Supramolecular Chirality Induction with Bisporphyrin Tweezer Receptors. Strong Metal Modulation of Effective Molarity Values

Inmaculada C. Pintre,[†] Simon Pierrefixe,[†] Alex Hamilton,[†] Virginia Valderrey,[†] Carles Bo,*[,†] and Pablo Ballester*[,†,‡]

[†]Institute of Chemical Research of Catalonia (ICIQ), Avgda. Països Catalans 16, 43007 Tarragona, Spain

[‡]Catalan Institution for Research and Advanced Studies (ICREA), Passeig Lluís Companys, 23, 08018, Barcelona, Spain

Supporting Information

ABSTRACT: We describe the synthesis of a bisporphyrin tweezer receptor **1**·H_4 and its metalation with Zn(II) and Rh(III) cations. We report the thermodynamic characterization of the supramolecular chirality induction process that takes place when the metalated bisporphyrin receptors coordinate to enantiopure 1,2-diaminocyclohexane in two different solvents, toluene and dichloromethane. We also performed a thorough study of several simpler systems that were used as models for the thermodynamic characterization of the more complex bisporphyrin systems. The initial complexation of the chiral diamine with the bisporphyrins produces a 1:1 sandwich complex that opens up to yield a simple 1:2 complex in the presence of excess diamine. The CD spectra associated with the 1:1 and 1:2 complexes of both metalloporphyrins, **1**·Zn_2 and **1**·Rh_2, display bisignate Cotton effects when the chirogenesis process is studied in toluene solutions. On the contrary, in dichloromethane solutions, only **1**·Zn_2 yields CD-active 1:1 and 1:2 complexes, while the 1:2 complex of **1**·Rh_2 is CD-silent. In both solvents, porphyrin **1**·Zn_2 features a stoichiometrically controlled chirality inversion process, which is the sign of the Cotton effect of the 1:1 complex is opposite to that of the 1:2 complex. In contrast, porphyrin **1**·Rh_2 affords 1:1 and 1:2 complexes in toluene solutions with the same sign for their CD couplets. Interestingly, in both solvents, the signs of the CD couplets associated with the 1:1 sandwich complexes of **1**·Zn_2 and **1**·Rh_2 are opposite. The amplitudes of the CD couplets are higher for **1**·Zn_2 than for **1**·Rh_2. This observation is in agreement with **1**·Rh_2 having a smaller extinction coefficient than **1**·Zn_2. We performed DFT-based calculations and assigned molecular structures to the 1:1 and 1:2 complexes that explain the observed signs for their CD couplets. Unexpectedly, the quantification of the thermodynamic stability of the two metallobisporphyrin/diamine 1:1 sandwich complexes revealed the existence of interplay between effective molarity values (EM) and the strength of the intermolecular interaction (K_m; N···Zn or N···Rh) used in their assembly. The EM for the N···Rh(III) intramolecular interaction is 3 orders of magnitude smaller than that for the N···Zn(II) interaction, both of which are embedded in the same scaffold of the **1**·M_2 bisporphyrin receptor.

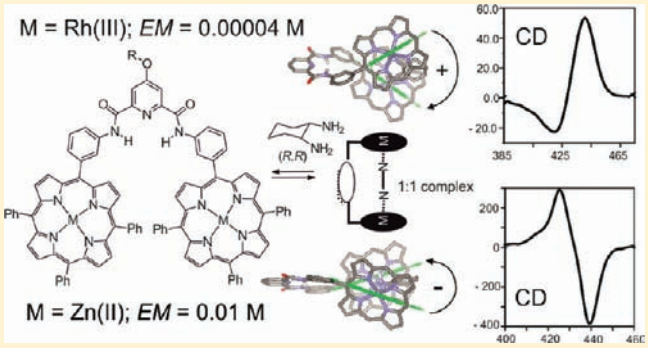

INTRODUCTION

Porphyrins feature a red shifted and very intense absorbance band ($\varepsilon \approx 4-5 \times 10^5$ M^{-1} cm^{-1}), known as the Soret or B band centered at ca. 420 nm, which makes them excellent chromophores for structural studies of exciton-coupled circular dichroism (CD).[1−3] If porphyrin chromophores experiencing exciton coupling are held in a chiral environment, that is, covalently connected to a chiral scaffold, the phenomenon can be clearly detected in the corresponding CD spectrum. A bisignate CD curve (so-called exciton couplet) is observed, with two bands of opposite sign and similar intensity centered around the λ_{max} of the UV−vis absorption corresponding to the transition dipoles. The sign of the couplet is determined by the absolute sense of the skewness (twist) of the interacting electric transition moments associated with the chromophores' transitions.[4,5] Evidence of exciton interaction between porphyrin chromophores can also be derived from spectral shifts or splitting in the Soret band of UV−vis spectra of composite systems compared to monoporphyrin. In the absorption spectrum, the magnitudes of the shifts and splitting are correlated with the relative orientation and distance between the coupled electric transition dipole moments associated with the Soret band. Employing a simplified model of single effective Soret transition moment per porphyrin unit,[6] the parallel orientation of coupled dipoles results in a blue shift of the Soret band since only excitation in the higher level energy level exciton state is allowed.

Received: November 22, 2011
Published: March 28, 2012

   dx.doi.org/10.1021/ic202515v | *Inorg. Chem.* 2012, 51, 4620−4635

The supramolecular application of the exciton-chirality rule with achiral bisporphyrin receptors (host) is based on the transfer of chirality from the chiral substrate (guest) to the resulting host–guest complex (chirogenesis); see Figure 1.

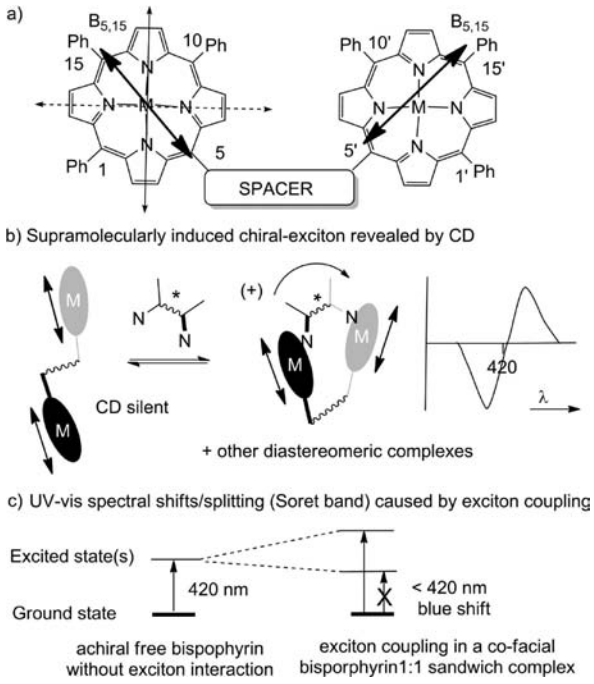

Figure 1. (a) Schematic representation of a bisporphyrin "tweezer" receptor. A simplified model with a single effective electric transition moment ($B_{5,15}$, double arrow in bold) is adopted for each porphyrin unit. The weight of the transverse $B_{1,10}$ component is reduced by fast rotation. (b) The exciton-chirality rule relates the sense of the torsion angle between the two coupled electric dipole moments of the bisporphyrin units of a 1:1 supramolecular chiral complex to the sign of the CD couplet. (c) Diagram of the origin of UV–vis spectral shifts due to exciton coupling.

In most of the examples described in the literature, the chiral guests contain two interaction sites. That is, the ligands are bidentate and capable of undergoing simultaneous axial coordination with the two metalloporphyrin binding units of the receptors. In other words, the achiral bisporphyrin receptors function as a molecular "tweezer" grabbing the guest in an open cavity defined by two porphyrin units bridged by a spacer.

The resulting ditopic 1:1 complexes are usually highly thermodynamically stable and constitute ideal systems for the calculation of effective molarity values (EM). EM values are used to quantify the ease of the intramolecular interaction.[7] The physical expression of chelate cooperativity is reflected in an increase in binding affinity for the ditopic 1:1 complex compared to the statistically corrected value of a monotopic 1:1 counterpart ($K_{1:1\text{ditopic}} > 4K_{1:1\text{monotopic}}$). The EM value is not in itself a measure of chelate cooperativity, but the different ways proposed for the assessment of such cooperativity do require EM calculation.[8−10] In general, the EM value is assumed to be an independent property of the supramolecular scaffold of the tweezer receptor. Thus, in a "tweezer"-like complex based on the same scaffold, one might expect that an increase in the strength of the intramolecular interaction (coordination bond, N···M) should produce a boost in the yield of the cyclic ditopic complex (EM × K_m). The two metallobisporphyrin systems (Rh and Zn) studied in this work have been shown to constitute a minimal platform to investigate these assumptions.

When chiral recognition (stereodifferentiation) is operative during the formation of the 1:1 "tweezer" complex, the chirality of the guest is transferred in the formation of one or a few diastereoisomeric complexes (stereospecific conformations) that are energetically more favorable than others. The diastereoisomeric complexes display chiral spatial arrangements with fixed relative orientations (twist) of the porphyrin units of the bound "tweezer". The close spatial proximity of the porphyrin cores encountered in the 1:1 chiral "sandwich" complexes induces exciton coupling between the porphyrins' electronic transitions.

In general, the CD and UV spectra experimentally observed represent a weighted average of corresponding spectra of the individual diastereoisomeric complexes in solution. Normally, the sign of the couplet inverts upon changing the absolute configuration of the chiral guest, and the observation of small CD signals are explained by partial cancellation of intense CD bands for diastereoisomeric complexes present in solution and having opposite couplet signs.

An important advantage of the exciton-chirality rule is its nonempirical nature. There are strong theoretical grounds, which also apply to bisporphyrin supramolecular complexes, to relate the observed sign of the CD couplet to the relative spatial orientation exhibited by the chromophores in the supramolecular chiral structure. Nowadays, ab initio calculations constitute an invaluable methodology to predict CD spectra from given supramolecular structures and become fundamental in the rationalization of the supramolecular chirogenesis processes.[11,12]

Achiral bisporphyrin tweezer[13,14] receptors are powerful tools for the absolute configurational analysis of organic compounds using CD spectroscopy.[15−17] Alternatively, related CD studies of bisporphyrin "tweezer" receptors binding chiral guests of known absolute configuration with the assistance of theoretical calculations are used to comprehensively investigate the various controlling factors (electronic and structural) that influence the chirogenic process and how they are affected by external and internal stimuli.[18]

In 2008, we reported the binding of bisporphyrin tweezer **1a**·Zn_2 with enantiopure 1,2-diaminocyclohexane **2** in dichloromethane solution (Scheme 1).[19] The system expressed the properties of both chirality induction and stoichiometrically controlled inversion. A related finding had already been reported by Borovkov et al. with a simpler ethane bridged bisporphyrin receptor.[20] We undertook the work reported here in order to investigate in more detail the influence of the metal center and solvent on the chirality induction and inversion processes displayed by the complexation of **1**·M_2 tweezers with enantiopure diamine **2**. We also wanted to combine the experimental results with electronic structural methods in the assignment of molecular structures to the **1**·M_2⊃*R*,*R*-**2** (1:1) and **1**·M_2@(*R*,*R*-**2**)$_2$ complexes formed during the binding process. This endeavor constitutes a necessary step to achieve a rationalization of the observed chirality transfer and inversion on the basis of electronic and structural factors.

Among the different metals that can be inserted into the porphyrin core, we were interested in investigating iodo-Rh(III) tweezer receptors. To the best of our knowledge, there are no reports of supramolecular chirality induction with Rh(III) porphyrins. Halogenorhodium(III) porphyrins are diamagnetic, and they generally bind a single amine on the

dx.doi.org/10.1021/ic202515v | *Inorg. Chem.* 2012, 51, 4620–4635

Scheme 1. Synthesis and Structures of the Porphyrins Used in This Study[a]

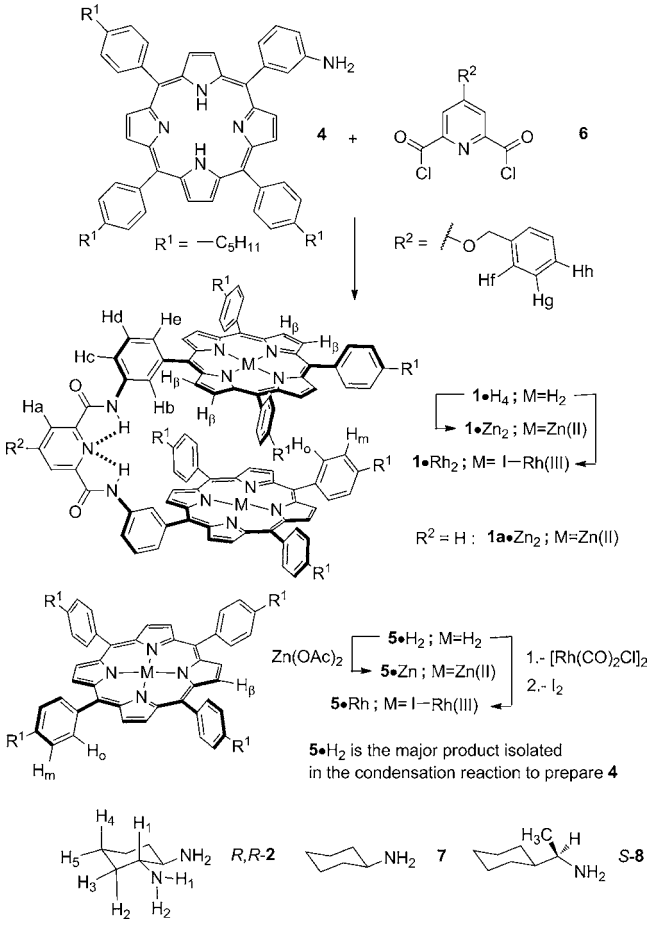

[a]The line drawing structures of the amines used in the study are also shown at the bottom of the scheme.

axial site trans to the halogen atom featuring a high binding affinity and very slow dissociation kinetics.[21] Halogenorhodium(III) porphyrins can be envisaged as structural analogues of Zn-porphyrins providing thermodynamically and kinetically more stable supramolecular assemblies based on ligand axial coordination chemistry with amines. As mentioned above, the extraction of EM values from the thermodynamic stability constants calculated for 1:1 Zn(II) and Rh(III) "tweezer"-like complexes will constitute a real test for the general assumption that EM values can be extrapolated among analogous supramolecular structures independently of the strength of the intermolecular interactions. In addition, we found that reports on the thermodynamic properties of covalently linked Rh(III) porphyrin dimers are relatively scarce,[22] although Rh(III) monoporphyrins have received attention for the construction of mono- and multimetallic oligoporphyrin systems through axial coordination with ligands,[23−27] as receptors for amino acid/esters[21,28,29] or nucleobases, as chemical shift chiral reagents for amines,[30] and even in the template synthesis of rotaxanes.[31]

RESULTS AND DISCUSSION

Synthesis of Porphyrins and Structural Considerations. Aminoporphyrin **4** was prepared according to methods described in the literature.[32] We note that the major product of the condensation reaction used to prepare porphyrin **4** is tetraalkylphenylporphyrin **5**·H_2. 5-Benzyloxy-2,6-pyridine dicarbonyl chloride **6** was prepared in four steps following a previously published procedure.[33,34] Coupling of aminoporphyrin **4** was accomplished by cannulating a solution of diacid chloride **6** in methylene chloride into a solution containing 2.4 equiv of the porphyrin and excess triethylamine. Column chromatography of the crude products allowed the recovery of unreacted porphyrin and the isolation of bisporphyrin **1**·H_4 as a purple solid in 61% yield. Metalation with Zn(II) was accomplished in almost quantitative yield by using a solution of zinc acetate in CH_2Cl_2/MeOH (3:1), yielding pure Zn-monoporphyrin **5**·Zn and Zn-bisporphyrin **1**·Zn_2 after column chromatography purification with basic alumina. Metalation of the free base porphyrins **5**·H_2 and **1**·H_4 with a chlorodicarbonylrhodium(I) dimer, followed by in situ oxidation with iodine and purification by column chromatography with neutral alumina, afforded the diamagnetic iodorhodium(III) porphyrins **5**·Rh and **1**·Rh_2 in approximately 85% yield.

The ^{1}H NMR spectra of the metalated monoporphyrins **5**·Zn and **5**·Rh when dissolved in CH_2Cl_2-d_2 or toluene-d_8 show sharp and well-defined signals that are easily assigned. We observed two pair of doublets for the protons of the *meso*-phenyl substituents in **5**·Rh, indicating slow rotation of the C_{meso}−C_{phenyl} bond on the ^{1}H NMR time scale and confirming that the two porphyrin faces are not chemically equivalent. The proton signals characteristic of an axially coordinated methanol molecule in the opposite face of the axial iodo ligand could also be detected.[23] Single crystals of **5**·Rh·MeOH suitable for X-ray diffraction analysis were grown from a dichloromethane/methanol solvent mixture. Two crystalographically inequivalent molecules of **5**·Rh·MeOH are present in the asymmetric unit of the crystal (Figure 2). A packing plot shows that the molecules stacked on one another confronting the iodo ligand with the coordinated methanol and forming a tilted columnar arrangement. The planes of adjacent porphyrin units in the stack are rotated 36° with respect to each other, whereas the porphyrin planes of alternate units are parallel.

The ^{1}H NMR spectra of the bisporphyrins **1**·Zn_2 and **1**·Rh_2 when dissolved in CH_2Cl_2-d_2 (dielectric constant, dipolar moment; 9.1, 1.6 D), $CHCl_3$-d (4.8, 1.04 D), or toluene-d_8 (2.4, 0.36 D) show broad and unresolved proton signals, suggesting the existence of aggregation processes or processes of interconversion between conformers with exchange rate constants that are intermediate on the ^{1}H NMR chemical shift time scale (Figure 3). On the contrary, when bisporphyrins **1**·Zn_2 and **1**·Rh_2 are dissolved in THF-d_8 (7.5, 1.75 D), ^{1}H NMR spectra with sharp and well-resolved proton signals are observed. This result suggests that the broadening of the proton signals observed in the nonoxygenated solvents is probably due to aggregation processes induced by $\pi-\pi$ interactions between the porphyrin rings. Because the polar properties (dielectric constant and dipolar moment) of THF and CH_2Cl_2 are similar, it is likely that the oxygen atom in the THF molecule coordinates to the metal center, disrupting these intermolecular interactions. The aggregation behavior of the bisporphyrin **1**·Rh_2 was evidenced by a significant red shift of their Soret band during dilution experiments in TOL solution in the range of concentrations of 10^{-5}−10^{-7} M (Supporting Information). The position of the porphyrin's Soret band remained constant at concentrations below 0.1 μM. The mathematical analysis of the dilution data assuming a simple dimerization process afforded K_d = 1.6 × 10^5 M^{-1}. In addition, the aggregation

dx.doi.org/10.1021/ic202515v | Inorg. Chem. 2012, 51, 4620−4635

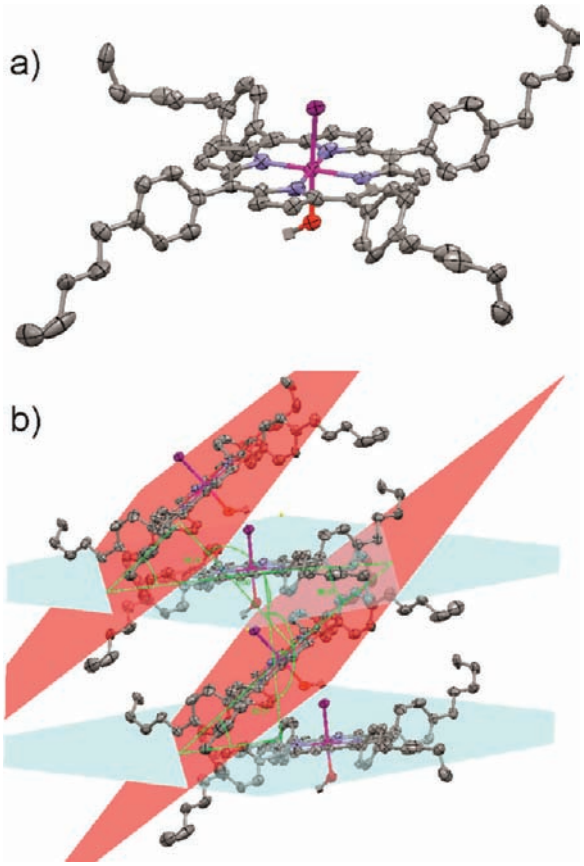

Figure 2. (a) Solid-state structure of **5**·Rh·MeOH. (b) Packing of **5**·Rh·MeOH in the solid state. Calculated planes defined by the four nitrogen atoms of the porphyrin rings are shown highlighting the relative orientation of the units in the stack. Hydrogen atoms have been removed for clarity. All atoms in the porphyrin structure are shown as thermal ellipsoids.

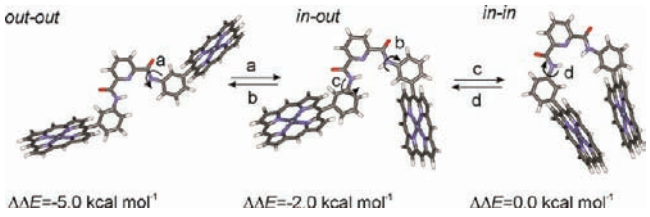

Figure 3. DFT-optimized structures for the conformers of structurally simplified bisporphyrins related to **1**·M_2 and proposed interconversion equilibria in which they are involved.

properties of Zn-bisporphyrins analogous to **1**·Zn_2 have already been reported, and for TOL solution, dimerization constant values on the order of 5×10^3 M^{-1} were calculated.[35] In DCM solution, the aggregation process is sensibly reduced (i.e., $K_d \approx 3 \times 10^2$ M^{-1} for **1**·Zn_2) and completely eliminated, for both **1**·Zn_2 and **1**·Rh_2, if THF is used as solvent (Supporting Information).

We intentionally employed spacer **6** as a mean to restrict the conformational freedom of bisporphyrins **1**·M_2.[36] The internal hydrogen bonds present in the 2,6-dicarboxamidopyridine unit force the spacer to predominantly adopt a syn-syn conformation. However, the free rotation that still exists around the NH−$C_{meta\text{-}meso\text{-}phenyl}$ in **1**·M_2 enables the existence of at least three different conformers incorporating the original preorganization motif.

A simplified analogue of bisporphyrin **1a**·Zn_2, in which three *meso*-phenyl substituents in each porphyrin unit and the benzyl ether in the linker are removed, was used to compute the gas-phase energy of three conformers. Structures of the conformers were optimized by the method described in the computational details (Supporting Information). The calculations show a 5 kcal mol^{-1} energy preference for the *out-out* conformation. The *in-out* conformation is 3 kcal mol^{-1} less stable than the *out-out* conformation. This result suggest that, in the gas-phase, bisporphyrin **1a**·Zn_2 adopts an *out-out* conformation almost exclusively.

The ^{1}H NMR spectrum of **1**·Zn_2 in THF-d_8 shows a single set of proton signals, implying either that **1**·Zn_2 is present in solution as a single conformer, probably in the *out-out* conformation based on previous calculation results, or that the interconversion between conformers is fast on the NMR time scale (Figure 4). On the other hand, the ^{1}H NMR spectrum of **1**·Rh_2 in THF-d_8 displays multiple signals for the same type of protons, that is, NH, *β*-pyrrole, *meso*-phenyl aromatics, or benzylic CH_2. We ascribe this different behavior to a slow rotation on the NMR time scale of the C_{meso}−$C_{amidophenyl}$ bond in the porphyrin units of **1**·Rh_2 that have chemically nonequivalent faces. This slow rotation provides additional conformers in equilibria with any of the three basic conformations that **1**·Rh_2 can adopt with respect to the relative spatial orientation of its porphyrin units (*in-in*, *out-out*, or *in-out*; see Figure 3). As mentioned above, the similar dynamic behavior observed with monoporphyrin **5**·Rh doubled the number of the signals of *meso*-phenyl protons.

To substantiate the chemical integrity of **1**·Rh_2, we investigated its complexation with the symmetric ditopic diamine DABCO (1,4-diazabicyclo(2,2,2)octane) using ^{1}H NMR spectroscopy at millimolar concentrations. The addition of incremental amounts of DABCO to the solution of **1**·Rh_2 in THF-d_4 produces the appearance of a new set of sharp proton signals that grew at the expense of the multiple protons signal of free **1**·Rh_2 (Figure 5). We allocate the new set of signals to the sandwich 1:1 complex **1**·Rh_2⊃DABCO. Diagnostic signals for the protons of the DABCO sandwiched guest are observed at $\delta = -5$ ppm. When 1 equiv of DABCO is added, only the set of new proton signals is observed. The assignment of the new set of signals to the protons of bound bisporphyrin is simple, indicating that the ditopic coordination of DABCO locks bisporphyrin **1**·Rh_2 into the cofacial conformer and confirms the chemical integrity of the sample. The 1:1 sandwich complex **1**·Rh_2⊃DABCO is highly thermodynamically stable and, even at a millimolar concentration, does not open up in the presence of excess DABCO (3.6 equiv).

Thermodynamic Characterization of Model Complexes. Before examining the induced chirality transfer of enantiopure 1,2-diaminocyclohexane **2** to bisporphyrins **1**·Zn_2 and **1**·Rh_2, we investigated the binding properties of simpler systems that cannot assemble into intramolecular sandwich complexes. The values of the binding interactions derived from the latter will be used as references or standards for the relevant binding interactions that occur in the former. The binding models used in the fit of the titration data derived from the model complexes are described in detail in the Supporting Information.

Determination of Microsocopic Binding Constants for the Interactions R-NH_2···Zn(II) and R-NH_2···Rh(III)-I. The coordination of monoamine **7** (cyclohexylamine) with monoporphyrin **5**·Rh was probed by UV−vis titrations in toluene (TOL),

dx.doi.org/10.1021/ic202515v | *Inorg. Chem.* 2012, 51, 4620−4635

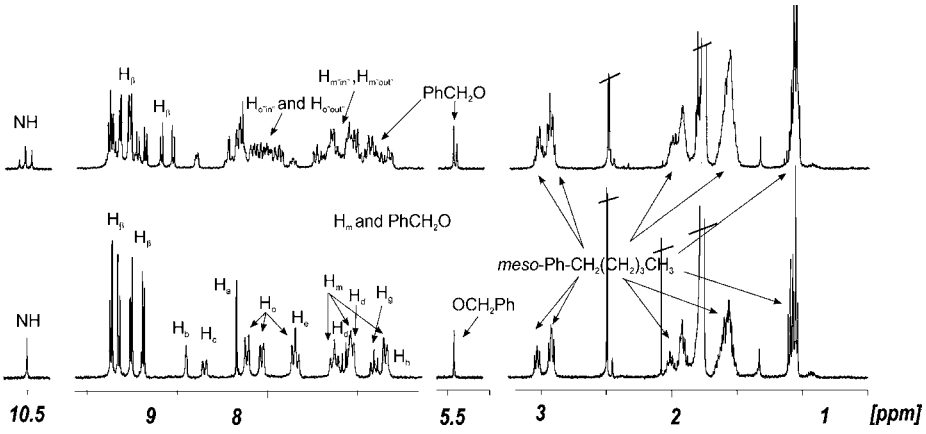

Figure 4. ^{1}H NMR spectra of **1**·Rh_2 and **1**·Zn_2 in THF-d_8 solution. See Scheme 1 for proton assignment. Please notice that the two ortho and meta protons in each *meso*-phenyl substituent in **1**·Rh_2 are chemically nonequivalent (different substitution of the two faces of the porphyrin unit) and split into four different signals as a result of the slow rotation in the NMR time scale of the $C_{meso}-C_{phenyl}$ bond.

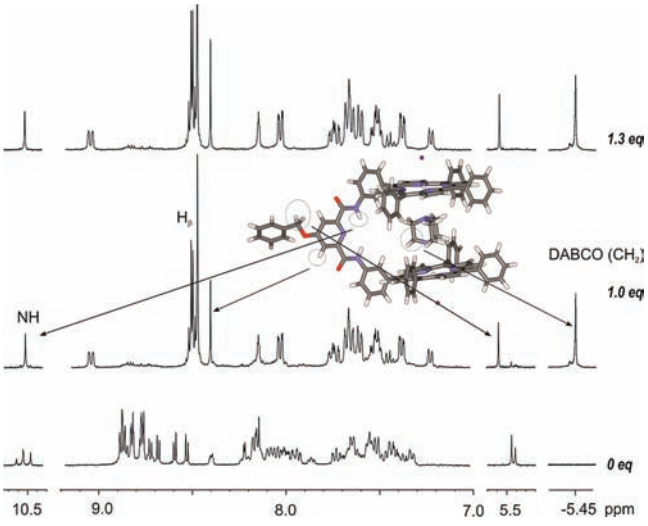

Figure 5. Downfield and upfield selected regions of the ^{1}H NMR spectra of **1**·Rh_2 in THF-d_8 solution with increasing amounts of DABCO. The inset shows the energy-minimized molecular structure of the sandwich complex **1**·Rh_2⊃DABCO. The complex is stable in the presence of more than 1 equiv of DABCO. The small signals resonating in the region of 8.6–8.8 ppm after the addition of 1.3 equiv of DABCO are impurities. See the Supporting Information for a detailed proton assignment.

showing a shift of the Soret band from 415 to 432 nm (see the Supporting Information). We assigned the 17 nm shift to the formation of the 1:1 axially coordinated complex **5**·Rh@7. Analysis of the binding isotherm using a 1:1 binding model (Scheme S3a, Supporting Information) demonstrated that the binding constant is too high to be measured accurately at this concentration ([**5**·Rh] = 5.8×10^6 M]). Thus, we simply estimated the binding constant value of $K_{1:1}$ (**5**·Rh@7) as 1×10^8 M^{-1} and assigned a similar value to the reference microscopic constant K_m for the interaction R-NH_2···Rh(III)-I in toluene.[37] The formation of 1:1 complexes between Rh(III) porphyrins and amines having high thermodynamic stability and even surviving column chromatography was previously reported by Sanders[22] and Aoyama.[29]

Similarly, we investigated the complexation of cyclohexylamine **7** with **5**·Zn in TOL. During the titration, **5**·Zn experienced a shift of the Soret band from 424 to 431 nm. A shift of 7–10 nm is characteristic for the formation of 1:1 axial complexes of amines with Zn porphyrins. The mathematical analysis of the titration data using the 1:1 binding model allowed the accurate calculation of a binding constant value $K_{1:1}$ (**5**·Zn@7) = $1.0 \pm 0.2 \times 10^4$ M^{-1} that we assigned to the microscopic interaction of R-NH_2···Zn(II) in TOL. We had previously also determined the value of $K_{1:1}$ (**5**·Zn@7) in dichloromethane (DCM) solution as 5.0×10^4 M^{-1}.[19] This result indicates a 5-fold reduction in the value of the microscopic binding constant determined in the aromatic solvent TOL compared to DCM.

Calculation of the Cooperativity Factor for the Bisporphyrin **1**·Zn_2. As mentioned above, bisporphyrins **1**·Zn_2 and **1**·Rh_2 seem to aggregate at micromolar concentrations in TOL. Dilution studies in the concentration range of 10^{-6}–10^{-7} M^{-1} showed no evidence of this behavior for **1**·Zn_2 in both solvents and a reduced aggregation process operating for **1**·Rh_2 below 1 μM concentration in TOL solutions. We studied the binding of monoamine **7** with bisporphyrin **1**·Rh_2 in TOL and DCM and with bisporphyrin **1**·Zn_2 in TOL using spectrophotometric titrations. (See Scheme S4, Supporting Information, for the detailed binding model.) The titrations of **7** with **1**·Zn_2 and **1**·Rh_2 were nonisosbestic. Probably, the nonisosbestic behavior reflects small differences in the binding properties of the 1:1 and 2:1 complexes. In all cases, the titration data were analyzed by considering three colored states for the bisporphyrin (free, 1:1, and 2:1).

On the one hand, the fit of the titration data of **1**·Zn_2 with **7** allowed the calculation of reliable stability constant values for the complexes 1:1 $K_{1:1}$(**1**·Zn_2@7) and 1:2 $K_{1:2}$(**1**·Zn_2@7_2), as well as their corresponding UV-spectra. The microscopic constant value derived for the R-NH_2···Zn(II) interaction using the equation $K_{m2} = 2K_{1:1\leftrightarrow1:2}$ is very close to the value we obtained in the titration of monoporphyrin **5**·Zn with minomaine **7** ($1.0 \pm 0.2 \times 10^4$ M^{-1}). However, the microscopic constant for the same interaction when derived from the relationship $K_{m1} = K_{1:1}/2$ is slightly smaller. This result indicates a decrease in the binding affinity of the first interaction of **1**·Zn_2 with **7** compared to the strength calculated for the model system (**7** with monoporphyrin **5**·Zn). This small anticooperative behavior, possibly produced by an interaction with the adjacent porphyrin unit in **1**·Zn_2, was quantified by a cooperativity factor $\alpha_P = 0.5$ calculated from the ratio of stepwise binding constants $K_{1:1}$(**1**·Zn_2@7)/$K_{1:1\leftrightarrow1:2}$ (**1**·Zn_2@7_2) = $4\alpha_P$ (Scheme S4,

dx.doi.org/10.1021/ic202515v | *Inorg. Chem.* 2012, 51, 4620–4635

Supporting Information). We derived a similar value for α_P in a closely related Zn bisporphyrin in the complexation with quinuclidine.[36] On statistical grounds, the expected value of α_P for truly independent binding sites is 1.0; on the basis of our definition of α_P, smaller numbers correspond to the anticooperative behavior of the two porphyrin units.

On the other hand, the mathematical analyses of the titration data of bisporphyrin **1**·Rh_2 with **7**, in either TOL or DCM, were carried out in a completely different manner. We fixed the stability constants of the complexes to their statistically estimated values using the relationships $K_{1:1} = 2\alpha_P K_m$ and $K_{1:2} = \alpha_P K_m^2$ ($K_m = 1 \times 10^8$ M^{-1} in TOL and 5×10^8 M^{-1} in DCM). As determined for Zn-porphyrins **5**·Zn and **1**·Zn_2, we assumed here that, for bisporphyrin **1**·Rh_2, the K_m value also displays a 5-fold increase when moving from TOL to DCM. We also assigned a cooperativity factor of 0.5 to **1**·Rh_2 based on the results obtained with **1**·Zn_2. The UV−vis spectra of the three species were the only variables considered during the fitting procedure. For the two solvents, we obtained a very good fit of the titration data to the theoretical binding isotherms. In addition, the UV−vis spectra calculated for the three species, in which **1**·Rh_2 is involved, displayed the spectral features expected for their stoichiometry and geometry (see the Supporting Information). These observations give some indication of the quality and correctness of the data analysis, as well as the values statistically estimated as lower limits for the stability constants of the complexes, which, in turn, were derived from our estimate of the microscopic binding constant for the R-NH_2···Rh(III)-I.

Calculation of the Cooperativity Factor for the R,R-2 Diamine. Next, we calculated the cooperativity factor for the ditopic chiral diamine *R,R*-**2** in both solvents, DCM and TOL. We used titrations performed at millimolar concentrations with monoporphyrins **5**·Zn and **5**·Rh using ^{1}H NMR spectroscopy. In DCM at 298 K, the system **5**·Rh and *R,R*-**2** displayed slow exchange on the NMR time scale. Proton signals for free **5**·Rh, the 2:1 (porphyrin/amine) complex, and the 1:1 complex could be assigned (Figure 6). In the presence of less than 0.5 equiv of *R,R*-**2**, only free **5**·Rh and (**5**·Rh)$_2$⊃*R,R*-**2** were observed in slow exchange. When 0.5 equiv of *R,R*-**2** is added, (**5**·Rh)$_2$⊃*R,R*-**2** is the exclusive species in solution. The addition of more than 0.5 equiv of *R,R*-**2** provoked the observation of separate proton signals for (**5**·Rh)$_2$⊃*R,R*-**2** (2:1) and **5**·Rh@*R,R*-**2** (1:1) complexes. As the concentration of *R,R*-**2** increased, the equilibrium gradually shifted in favor of the 1:1 complex. The signal of the *β*-pyrrole protons in the 2:1 sandwich complex was shifted upfield relative to the corresponding signal in free **5**·Rh or bound in the 1:1 complex. This is due to the proximity of the two porphyrin rings in the 2:1 sandwich complex, causing a large ring-current-induced shift. The two ortho and meta protons of the *meso*-phenyl substituents in free **5**·Rh and in its complexes are chemically nonequivalent and split in two doublets due to nonequivalent faces of the porphyrin unit together with slow rotation on the NMR time scale of the $C_{meso}-C_{p\text{-phenyl}}$ bond (vide supra).

In the upfield region of the ^{1}H NMR spectra, the behavior of the signals of the protons for the bound diamine *R,R*-**2** is in agreement with the observations made in the aromatic region of the spectra for the *β*-pyrrole protons. Until 0.5 equiv of diamine is added, the observed proton signals for the bound diamine correspond to the (**5**·Rh)$_2$⊃*R,R*-**2** (2:1) complex. Upon addition of increasing amounts of *R,R*-**2**, a new set of proton signals start to appear, corresponding to the **5**·Rh@*R,R*-**2** (1:1)

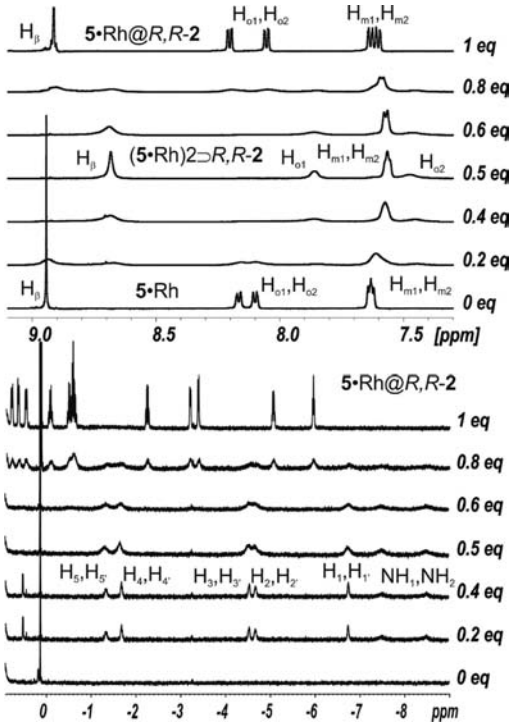

Figure 6. Downfield and upfield regions of ^{1}H NMR spectra acquired during the titration of **5**·Rh with *R,R*-**2** in CH_2Cl_2-d_2. Top: proton signals for the *β*-pyrrole and ortho and meta *meso*-phenyl protons in free and 1:1 and 2:1 complexes are indicated in the downfield expansion. Bottom: upfield expansion showing separate signals for the protons of the *R,R*-**2** diamine in the 1:1 (assigned) and the 2:1 complexes (not assigned). See Scheme 1 for proton assignment. Whereas the protons of the bound *R,R*-**2** amine in the C_2 symmetric 2:1 complex appear as 8 different signals, each one containing two chemically, but not magnetically, equivalent protons, the same protons in the nonsymmetric 1:1 complex should give rise up to 16 different signals.

complex. The observation of separate proton signals for the two complexes of different stoichiometry indicates that they are involved in slow chemical exchange on the ^{1}H NMR time scale. When 1 equiv of diamine is added, the **5**·Rh@*R,R*-**2** (1:1) complex is the only species present in solution. The higher symmetry (C_2) of the (**5**·Rh)$_2$⊃*R,R*-**2** (2:1) complex compared with that of **5**·Rh@*R,R*-**2** (1:1) becames apparent from the analysis of the number of proton signals of the bound diamine in the two respective states.

The association constants for the 1:1, **5**·Rh@*R,R*-**2**, and 2:1, (**5**·Rh)$_2$⊃*R,R*-**2**, complexes are too high to be measured accurately at NMR concentration. However, the value of the cooperativity factor α_L can be calculated using the following relationship, $K_{2:1\leftrightarrow 1:1} = 4/\alpha_L$ (Scheme S3b, Supporting Information), where $K_{2:1\leftrightarrow 1:1}$ is the equilibrium constant of the destruction of the 2:1 sandwich complex to produce the 1:1 complex. The value of $K_{2:1\leftrightarrow 1:1}$ was calculated from the integration of the resonances of each of the two complexes after 0.5 equiv of diamine was added, and a value of $\alpha_L = 0.05$ was determined. This value indicates that the two nitrogen atoms of the diamine *R,R*-**2** experience a severe anticooperative behavior upon coordinating to two porphyrin units.

For the systems **5**·Rh with *R,R*-**2** in TOL and **5**·Zn with *R,R*-**2** in both TOL and DCM solutions, we observed fast chemical exchange on the NMR time scale between free and bound species. The reduction in kinetic stability detected for the Zn

dx.doi.org/10.1021/ic202515v | *Inorg. Chem.* 2012, 51, 4620−4635

Table 1. Calculated and Estimated Macroscopic Binding Constants Derived from the Model Systems

porphyrin	ligand	solvent	$K_{1:1}$ [10^5 M^{-1}]	$K_{1:2}$(**1**·M_2) $K_{2:1}$(**5**·M) [10^9 M^{-2}]	$K_{1:1\leftrightarrow1:2}$(**1**·$M_2$)^b $K_{1:1\leftrightarrow2:1}$(**5**·M)^b [$10^5$ M^{-1}]
5·Rh	**7**	TOL	1000[c]		
5·Zn	**7**	TOL	0.1 ± 0.02		
5·Zn	**7**	DCM	0.5 ± 0.1[a]		
1·Zn_2	**7**	TOL	0.14 ± 0.06[a]	0.093 ± 0.008[a]	0.06 ± 0.002
1·Zn_2	**7**	DCM	1.2 ± 0.5[a]	4.5 ± 0.5[a]	0.4 ± 0.1
1·Rh_2	**7**	TOL	1000[c]	5 × 10^6[c]	
1·Rh_2	**7**	DCM	5000[c]	125 × 10^6[c]	
5·Rh	*R,R*-**2**	TOL	2000[c]	1 × 10^5 ± 0.2 × 10^5	5 ± 1
5·Rh	*R,R*-**2**	DCM			
5·Zn	*R,R*-**2**	TOL	0.2[c]	0.005	0.0025
5·Zn	*R,R*-**2**	DCM	1.0[c]	0.079	0.0079

[a]Values taken from refs 19 and 36. [b]$K_{1:1\leftrightarrow1:2} = K_{1:2}/K_{1:1}$ for **1**·M_2 and $K_{1:1\leftrightarrow2:1} = K_{2:1}/K_{1:1}$ for **5**·M. [c]Statistically estimated; see text for details.

Table 2. Microscopic Binding Constants for the M···N Interaction and Cooperativity Factors for the Ditopic Ligand *R,R*-2 and Bisporphyrins 1·M_2

porphyrin	ligand	solvent	K_{m1} [10^5 M^{-1}]	K_{m2} [10^5 M^{-1}]	α_P[d]	α_L
5·Rh	**7**	TOL	1000[a]			
5·Zn	**7**	TOL	0.1[a]			
5·Zn	**7**	DCM	0.5[a]			
1·Zn_2	**7**	TOL	0.07 ± 0.003[b]	0.13 ± 0.06[c]	0.5 ± 0.2	
1·Zn_2	**7**	DCM	0.6 ± 0.2[b]	0.7 ± 0.3[c]	0.8 ± 0.3	
5·Rh	*R,R*-**2**	TOL				0.01[e]
5·Rh	*R,R*-**2**	DCM				0.05[f]
5·Zn	*R,R*-**2**	TOL				0.05[e]
5·Zn	*R,R*-**2**	DCM				0.03[e]

[a]$K_{m1} = K_{1:1}$. [b]$K_{m1} = K_{1:1}/2$. [c]$K_{m2} = 2K_{11\leftrightarrow21}$. [d]$\alpha_P = K_{1:1}/4K_{1:1\leftrightarrow1:2}$. [e]$\alpha_L = 4/K_{2:1\leftrightarrow1:1}$, where $K_{2:1\leftrightarrow1:1} = K_{1:1}/K_{1:1\leftrightarrow2:1}$. [f]Calculated from integration of the ^{1}H NMR signals.

system correlates well with the diminution of thermodynamic stability. Specifically, the microscopic binding constant calculated for the R-NH_2···Zn(II) is 4 orders of magnitude smaller than our estimate for the R-NH_2···Rh(III) interaction. The reduced kinetic stability observed for the rhodium complexes in TOL also reflects a decline in binding affinity in this solvent compared with DCM. This observation supports the supposition that the ratio between the microscopic constant values in both solvents that we derived from Zn-porphyrin titrations can be extrapolated to the Rh(III) analogues.

From the previous ^{1}H NMR titration experiment of **5**·Rh in DCM, we learned that, up to the addition of 0.5 equiv of *R,R*-**2**, the (**5**·Rh)$_2$⊃*R,R*-**2** sandwich complex is the species predominantly formed. When more than 0.5 equiv of *R,R*-**2** is added, the 2:1 complex, (**5**·Rh)$_2$⊃*R,R*-**2**, is destroyed to yield the 1:1 complex, **5**·M@*R,R*-**2**. For the systems in fast exchange, we determined the equilibrium constant for the destruction of the 2:1 complex, $K_{2:1\leftrightarrow1:1}$, from the ratio of the macroscopic stability constants of the two complexes, $K_{2:1\leftrightarrow1:1} = K_{2:1}/K_{1:1\leftrightarrow2:1}$. In turn, the stability constants of the complexes were determined by fitting the changes in chemical shifts recorded in NMR titrations to the corresponding binding model (1:1 and 2:1 complex formation). To reduce the number of variables during the fitting procedure, we fixed $K_{1:1}$ to the statistically estimated value $K_{1:1} = 2K_m$. At a low guest-to-host molar ratio, the ^{1}H NMR spectra of the titrations of the monoporphyrin **5**·Zn showed the existence of four highly upfield-shifted proton signals (Supporting Information). The relative integral ratio of these signals was 1:1:1:1, and their chemical shift values must correspond to the weighted average chemical shifts of some of the protons of *R,R*-**2** in the three different stoichiometric states experiencing fast chemical exchange in the NMR time scale. The increase in the concentration of *R,R*-**2** induces downfield shifts of the signals because the free and 1:1 complex states of the ligand become more populated. The chemical shift changes for the meso and *β*-pyrrolic protons are in agreement with those discussed for the system **5**·Rh with *R,R*-**2** in DCM but are rather involved in fast chemical exchange (Supporting Information). The determined α_L values for the diamine *R,R*-**2** in the systems experiencing fast exchange are on the same order of magnitude and also coincide with the α_L value calculated for the system **5**·Rh with *R,R*-**2** in DCM featuring slow chemical exchange. In conclusion, the two binding sites (nitrogen atoms) in diamine *R,R*-**2** show a markedly stronger anticooperative behavior than the two porphyrin units of the bisporphyrins **1**·M_2. The cooperativity factor values calculated for the ditopic ligand *R,R*-**2** and bisporphyrins **1**·M_2 also evidence a reduced solvent modulation effect. Tables 1 and 2 summarize the results derived from the model systems.

Molecular modeling studies assigned several binding geometries to the 2:1 sandwich complexes (**5**·M)$_2$⊃*R,R*-**2**. For example, Figure 7 depicts two CAChe-minimized structures for (**5**·Zn)$_2$⊃*R,R*-**2**; in both of them, the diamine *R,R*-**2** places the amino groups in an equatorial orientation. However, the axially coordinated porphyrin units adopt different spatial arrangements in trying to avoid steric crowding. Most likely, in solution, dynamic equilibria between different geometries of the complexes are at work.

Thermodynamic Equilibria Involved in the Binding of Ditopic Amine Ligand with Bismetalloporphyrins. At micromolar concentrations, the interaction of ditopic amines with bisporphyrins produces sandwich motifs encountered in

dx.doi.org/10.1021/ic202515v | *Inorg. Chem.* 2012, 51, 4620–4635

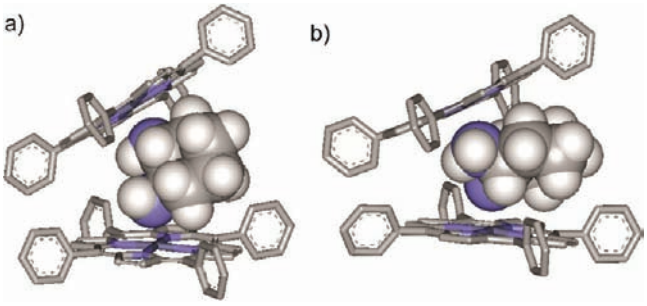

Figure 7. CAChe-minimized structures of different binding geometries for the 2:1 complex $(\mathbf{5}\cdot Zn)_2 \supset R,R\text{-}\mathbf{2}$: (a) The *R,R*-**2** ligand is sandwiched between two porphyrin units located at the edges of the ditopic guest. (b) The *R,R*-**2** ligand is sandwiched between two porphyrin units located on the top and bottom faces of the guest. **5**·Zn is shown as a stick representation. Hydrogen atoms and pentyl chains are removed for clarity. *R,R*-**2** is displayed as a CPK model.

intermolecular "ladders" or intramolecular "tweezer" complexes (Scheme 2). The intermolecular ladder-like complexes are

Scheme 2. Schematic Representation of the Possible Equilibria Involved in the Binding of a Bisporphryin with a Ditopic Diamine[a]

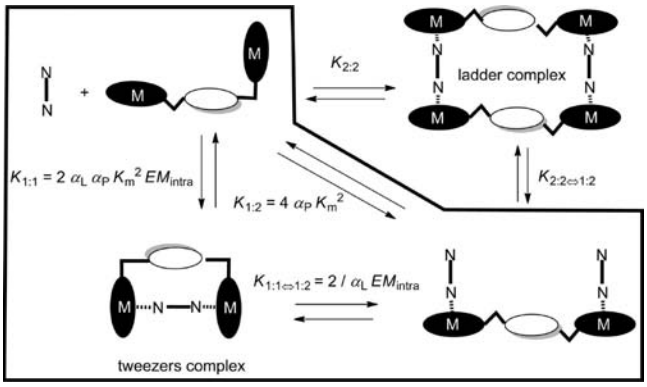

[a]EM is the effective molarity for the intramolecular interaction required for cyclization in the sandwich complex. Overall stability constants ($K_{1:2}$ and $K_{2:2}$) and stepwise equilibrium constants ($K_{1:1}$, $K_{1:1 \leftrightarrow 1:2}$, $K_{2:2 \leftrightarrow 1:2}$) are indicated. The relevant equilibrium constants for this study are related to K_m, EM, α_L, α_P, and statistical correction factors.

stable in the presence of a moderate excess of diamine, whereas the intramolecular sandwiches usually resist higher concentrations of diamine. Increasing the concentration of the amine finally breaks down the sandwich complexes, yielding 1:2 (porphyrin/amine) complexes. We demonstrated previously[19] that Zn-bisporphyrins, **1**·Zn_2, form exclusively 1:1 intramolecular sandwich complexes with ditopic amines that are shape- and size-complementary, that is, DABCO and *R,R*-**2** (*R,R*-1,2-diaminocyclohexane). For this reason, the formation of "ladder"-like complexes will not be considered in the binding model used to analyze the titration data of "tweezer" bisporphyrins **1**·M_2 with enantiopure 1,2-diaminocyclohexane described in the following sections.

Supramolecular Chirality Induction in the Coordination of Bisporphyrin Tweezer 1·Zn_2 with Enantiopure Ligand 2. We reported that the properties of chirality induction and inversion were both expressed and stoichiometrically controlled in the complexation of enantiopure 1,2-diaminocyclohexane **2** with Zn bisporphyrin **1a**·Zn_2 in DCM solution.[19] UV–vis titrations of **1**·Zn_2 with *R,R*-**2** revealed the initial formation of a thermodynamically stable 1:1 sandwich complex, **1**·$Zn_2 \supset R,R$-**2**, at low molar guest-to-host ratios. In the presence of excess diamine, the sandwich complex opened up to form a simple 2:1 complex, **1**·$Zn_2@(R,R\text{-}\mathbf{2})_2$. The sandwich complex, **1**·$Zn_2 \supset R,R$-**2**, displayed only a 2 nm red shift of the Soret band with respect to the maximum of free **1**·Zn_2. This is characteristic of sandwich complex formation in which the two porphyrin units of the tweezer are simultaneously bound to a ditopic ligand and experience strong exciton coupling between their transitions.[38] Interestingly, the CD titration revealed that the sandwich complex, **1**·$Zn_2 \supset R,R$-**2**, was endowed with a very strong (A = 783 M^{-1} cm^{-1}) negative exciton couplet. With respect to the higher stoichiometry 1:2 complex, **1**·$Zn_2@(R,R\text{-}\mathbf{2})_2$, the red shift of the Soret band was close to 10 nm, typical for open 1:2 bisporphyrin/amine. Quite unexpectedly, the mathematical analysis of the titration CD spectra assigned a weak (A = 139 M^{-1} cm^{-1}) positive bisignate signal to the **1**·$Zn_2@(R,R\text{-}\mathbf{2})_2$ complex, for which we had anticipated a silent CD. A direct visual analysis of the raw data obtained in the CD titration already made clear the existence of CD sign inversion when moving form low to high guest-to-host ratios.

Our previous studies with model systems evidenced a subtle influence of the solvent (DCM and TOL) in the microscopic binding constant value, K_m, for the $RNH_2\cdots Zn(II)$ interaction (Table 1). The K_m value is 5-fold higher in DCM than in TOL. It is probable that TOL better solvates the π-system of the porphyrin ring. We were interested in finding out how the reduction in binding affinity would be expressed in the chirogenesis process. We described above how we determined the α_p and α_L values for **1**·Zn_2 and *R,R*-**2**, respectively, using model systems, and we noticed that these values were almost not affected by changing the solvent. Consequently, they should not be responsible for alterations in the chirogenesis process upon a change in solvent.

First, we probed the interaction of **1**·Zn_2 with *R,R*-**2** using UV–vis titrations in TOL solution. The bisporphyrin concentration was maintained constant at ca. 1.25×10^{-6} M. The initial addition of *R,R*-**2** led to a shift of the Soret absorption band of 2 nm (422–424 nm) and a concomitant reduction of the half-bandwidth. This small 2 nm red shift is diagnostic of 1:1 ditopic bisporphyrin/diamine sandwich complexes experiencing exciton coupling.[39] Upon addition of more *R,R*-**2**, a new absorption appeared at 428 nm corresponding to the 1:2 open complex. As observed for the reference compound **5**·Zn, a Soret band shift of 10 nm is expected for axially coordinated complexes of Zn-porphyrins. The reduced red shift (6 nm compared with 10 nm) of the Soret band observed by the end of the titration could be indicative of a residual exciton in the 1:2 complex (Figure 8). The half-bandwidth of the final Soret band is noticeably smaller than that of the initial band and comparable with the one obtained after the initial additions. A reduction in the half-bandwidth suggests that the bisporphyrin adopts a preferred conformation and exhibits a reduction in conformational freedom. We did not observe any isosbestic point during the titration. This finding is in agreement with the existence of simultaneous multiple equilibria in the binding process. The titration data were analyzed using multivariate factor analysis and considering a binding model with three colorimetric stoichiometric states for **1**·Zn_2 (free, 1:1 and 1:2 complexes);

dx.doi.org/10.1021/ic202515v | *Inorg. Chem.* 2012, 51, 4620–4635

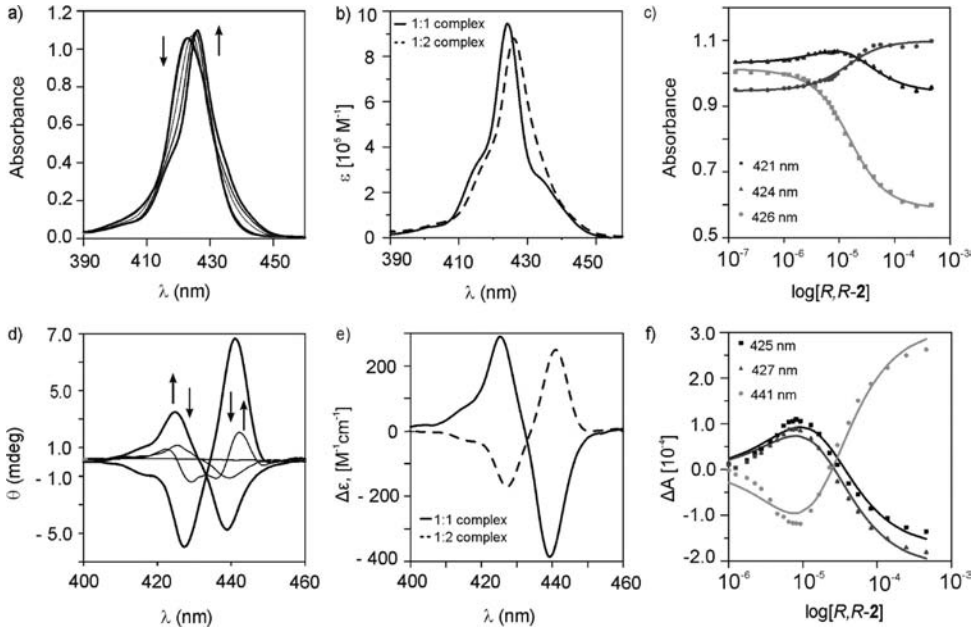

Figure 8. (a) UV−vis and (d) CD spectra obtained during the titration of **1**·Zn_2 and *R,R*-**2** in toluene solution at 298 K. The concentration of **1**·Zn_2 was maintained constant throughout the titration (1.25×10^{-6} M). The curves shown correspond to the addition of 0, 1.8, 7.4, 23.4, and 367 equiv of *R,R*-**2**. Calculated spectra for the 1:1 (continuous line) and 2:1 complexes (dashed line): (b) UV−vis (Soret band) and (e) CD. Fit of the titration data to the theoretical binding isotherm at selected wavelengths: (c) UV−vis and (f) CD.

see Scheme 2. The UV−vis spectra of free **1**·Zn_2 was fixed, and the fitting procedure returned the following values of $K_{1:1}$ = 6.7×10^4 M^{-1} and $K_{1:2}$ = 4.5×10^9 M^{-2}. The $K_{1:1}$ value determined for the 1:1 complex and its calculated spectrum are in support of the existence, to a certain extent, of a sandwich complex geometry with a ditopic interaction between the diamine and the bisporphyrin tweezers. Taken together, the results obtained are completely in agreement with the initial formation of a 1:1 complex displaying a sandwich-like geometry, which is destroyed by the addition of excess diamine, affording a 1:2 complex in which, surprisingly, residual exciton coupling and conformational bias are still present. Having determined the stability constant value of the 1:1 sandwich complex, we became interested in calculating its effective molarity (EM) using the relationship $K_{1:1} = 2\alpha_P\alpha_L K_m^2 EM$. The use of this equation implicitly assumes the formation of a single closed state for the 1:1 complex.[40] We determined a value of EM = 0.01 M for the 1:1 complex, indicating that the conformation adopted by the bisporphyrin is not highly strained. Similar values of EM (0.03 M) were calculated using DABCO as the ligand for a related bisporphyrin tweezer.[36]

When the interaction of **1**·Zn_2 and *R,R*-**2** was monitored using electronic CD spectroscopy, we observed that the initial addition of the amine led to the appearance and stepwise enhancement of a negative bisignate Cotton effect centered close to the maximum of the porphyrin Soret band. Nevertheless, the increase in concentration of *R,R*-**2** produced a rapid decrease in the initial ellipticity values of the sample and the generation of a more intense, but positive, CD couplet. We rationalize these results through the formation of an initial 1:1 complex **1**·Zn_2⊃*R,R*-**2** with reduced thermodynamic stability and associated with a negative couplet. The reduction in the strength of the intramolecular interaction Zn···N upon moving from DCM to TOL (5-fold reduction in K_m) produced a strong impact in the thermodynamic stability of the sandwich. The destruction of the 1:1 complex occurs simultaneously to its formation and produces a 1:2 complex **1**·Zn_2@$(R,R\text{-}\mathbf{2})_2$ possessing a positive couplet with an unexpectedly high amplitude. The analysis of the CD titration data fixing the values of the stability constants of the complexes to those calculated from the UV−vis titration allowed the calculation of the CD spectra for the two species (Figure 8e). The reasonable good fit observed between the experimental titration CD data and the theoretical binding isotherms supports the quality of the data analysis and of the predicted CD spectra.

In trying to assign a molecular structure to the 1:1 sandwich complex and rationalize the observed CD couplet by means of electronic and structural parameters, the low-energy geometries of the diastereoisomeric sandwich 1:1 complexes **1a**·Zn_2⊃*R,R*-**2** were investigated by DFT-based calculations. In Figure 7, we showed that, in a sandwich complex involving diamine *R,R*-**2** and two monoporphyrins, it is possible for the diamine to be oriented in at least two different arrangements. Similarly, the 1:1 complex **1a**·Zn_2⊃*R,R*-**2** could arrange the diamine in two possible geometries (Figure 9). Both structures of the 1:1 complex lead to calculated UV/vis and CD spectra in agreement with the experiments. However, the complex in which the amine adopts a parallel orientation with respect to the porphyrin rings is significantly higher in energy, approximately 10 kcal mol^{-1}, than the one in which the diamine is perpendicular to the porphyrin planes. Consequently, all further calculations consider the diamine placed in a perpendicular orientation.

The optimized structures and calculated UV−vis and CD spectra obtained from the DFT calculations of the two energy minima diastereoisomeric complexes, with the diamine oriented in a perpendicular arrangement, are shown in Figure 10. There is little energetic preference for either of the two different chiral diastereoisomeric complexes. In diastereoisomer **1a**·Zn_2⊃*R,R*-**2**-(-), the relative orientation of the "privileged" or effective electric transition moments,[6] $B_{5,15}$, which corresponds to the direction of the covalent linkage between the porphyrin and the

dx.doi.org/10.1021/ic202515v | *Inorg. Chem.* 2012, 51, 4620−4635

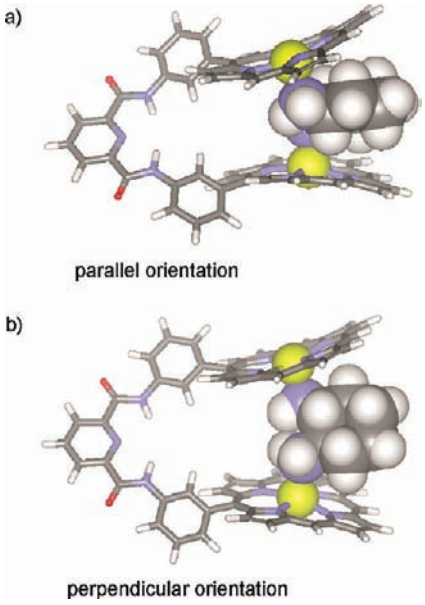

Figure 9. DFT-optimized structures of two different binding geometries for the 1:1 sandwich complex. (a) Parallel orientation of the diamine with respect to the porphyrin planes. (b) Perpendicular orientation of the diamine with respect to the porphyrin units. The parallel orientation of the diamine provides a 1:1 complex that is thermodynamically 10 kcal mol^{-1} less stable than the perpendicular one. Bisporphyrin **1a**·Zn_2 is shown as a stick representation and diamine **2** as a CPK model.

spacer (C-5/C-15), is anticlockwise with a dihedral angle of 34° between them. This diastereoisomer features a slightly more favorable energy (relative energy 0.6 kcal/mol) than the related diastereoisomer with a clockwise orientation of dipoles **1a**·Zn_2⊃*R,R*-**2**-(+). We assume that the effective transition picture is justified in bisporhyrin **1**·Zn_2 due to fast and unhampered rotation of the porphyrin units around the 5-15 axis.[41] The calculated energy difference translates in a 73% percentage preference ($K = e^{\Delta G/(-RT)} = 2.75$) for the **1a**·$Zn_2$⊃*R,R*-**2**-(-) in solution considering the exclusive formation of the two diastereoisomers under stoichiometric control (1:1). We are aware that this energy is in the range of experimental error in the calculations; nevertheless, according to the exciton-chirality method, the observed relative orientation between electronic transitions in the energy-minimized structure of **1a**·Zn_2⊃*R,R*-**2**-(-) nicely predicts the negative chirality observed experimentally. Furthermore, using the structure of **1**·Zn⊃*R,R*-**2**-(-) as input, the experimental electronic absorption and CD spectra are nicely reproduced by TD-DFT calculations at both the BP86/TZP and the SAOP/TZP levels. Structures for the 1·Zn⊃*S,S*-**2** complexes were also calculated. The lower energy structure for the **1a**·Zn_2⊃*S,S*-**2**-(+) diastereoisomer is very close to that of the enantiomer of **1a**·Zn_2⊃*R,R*-**2**-(-) and shows an energy preference of 0.6 kcal/mol with respect to the **1a**·Zn_2⊃*S,S*-**2**-(-) diastereoisomer of minimum energy. This result is in complete agreement with the fact that the experimental spectral and binding parameters obtained for *S,S*-**2** are identical to those of *R,R*-**2** within experimental error, except for the sign of the couplet, which is opposite.

We were also interested in assigning a molecular structure to the 1:2 complex produced by the destruction of the 1:1 complex in the presence of excess diamine. This high stoichiometry complex displayed chirality inversion with respect to its 1:1 precursor and an unexpectedly high amplitude of its CD spectra

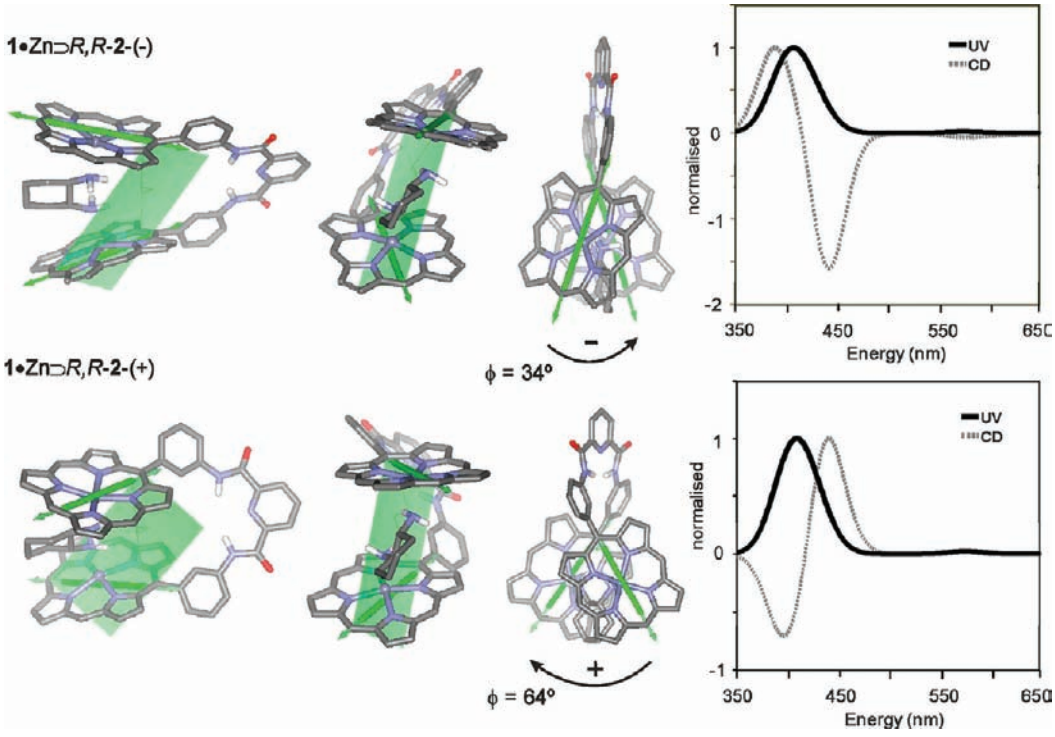

Figure 10. Side, front, and top views of the two energy-minimized diastereoisomeric 1:1 sandwich complexes **1a**·Zn_2⊃*S,S*-**2**-(-) and **1a**·Zn_2⊃*S,S*-**2**-(+). The plane defined by the atoms C-5, C5′, and C15′ is shown in all structures. The effective transition dipole moments of the porphyrin units are represented by green double arrows. The value of the dihedral angle between the two planes (C-15, C-5, C5′, C-15′) that contain the effective dipole moments and the predicted sign for the expected bisignate Cotton effect based on the exciton rule are indicated. Calculated UV–vis and CD spectra of the complexes are depicted.

dx.doi.org/10.1021/ic202515v | *Inorg. Chem.* 2012, 51, 4620–4635

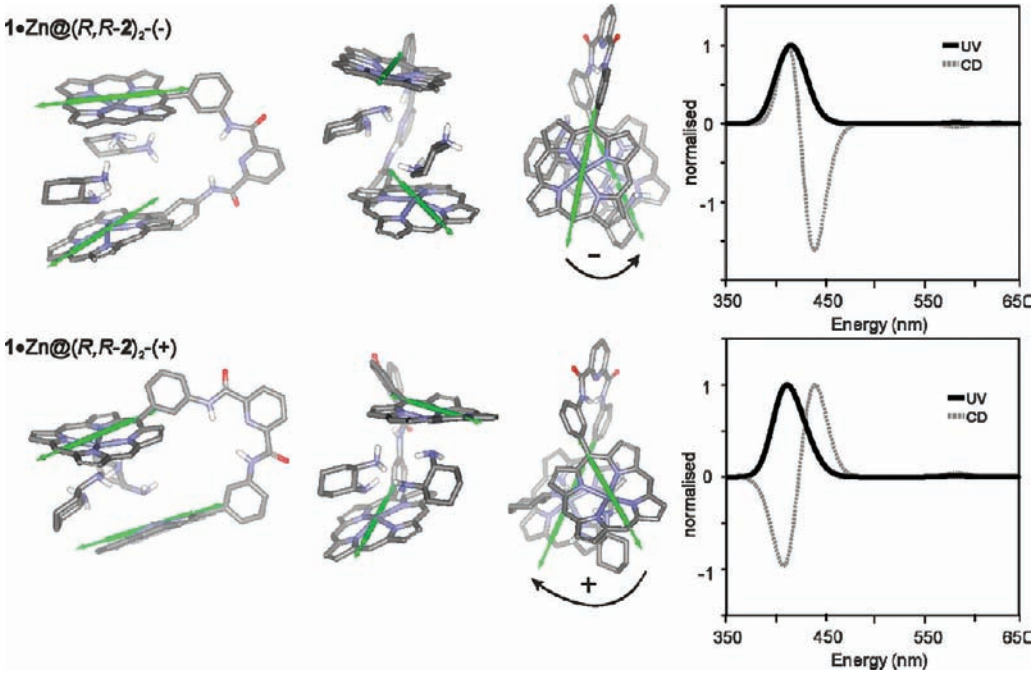

Figure 11. Side, front, and top views of the two energy-minimized diastereoisomeric 2:1 sandwich complexes **1a**·Zn_2@(*R*,*R*-**2**)$_2$-(-) and 1·Zn@(*R*,*R*-**2**)$_2$-(+). The effective transition dipole moments of the porphyrin units are represented by green double arrows. The predicted sign for the expected bisignate Cotton effect based on the exciton rule is indicated. Calculated UV−vis and CD spectra of the complexes are depicted.

especially in TOL solution. In addition, the UV−vis spectra of the 1:2 complex in DCM and more noticeably in TOL solution showed signs of the existence of residual exciton coupling between the porphyrin chromophores. That is, the maximum of the Soret band of the 1:2 complex was slightly blue shifted (418 nm) with respect to the absorption maximum (420 nm) provided by a model system consisting of monoamine **7** axially coordinated to monoporphyrin **5**·Zn. Molecular modeling studies suggested that the observed residual exciton coupling between the porphyrin chromophores in the 1:2 **1a**·Zn_2@(*R*,*R*-**2**)$_2$ complex could be the result of the establishment of intramolecular interactions between the two axially coordinated ditopic amines **2**. Different chiral monoamines we assayed, that is, *S*-**8**, did not give rise to 1:1 or 1:2 CD-active complexes; thus, the ditopic nature of the ligand seems to be fundamental to yield CD activity. Figure 12 shows the DFT-optimized structures

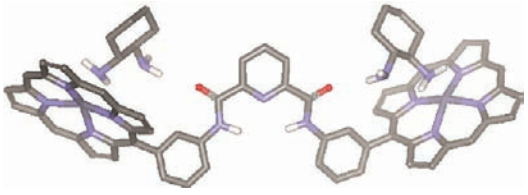

Figure 12. DFT-optimized structure for the *out-out* conformer of the 1:1 complex **1a**·Zn_2@(*R*,*R*-**2**)$_2$.

for two diastereoisomeric complexes **1a**·Zn_2@(*R*,*R*-**2**)$_2$ with the sense of the twist between the effective transition dipole moments of the porphyrin rings reversed. The calculated energy difference between **1a**·Zn_2@(*R*,*R*-**2**)$_2$-(+) and **1a**·Zn_2@(*R*,*R*-**2**)$_2$-(-) is 2.6 kcal mol^{-1} in favor of the former. Probably, the 1:2 complex adopts the *in-in* conformation as a consequence of the formation of intramolecular hydrogen bonds between the NHs and the nitrogen atoms of the two adjacent bound *R*,*R*-**2** ligands. In general, amines are poor hydrogen-bond donor groups; we propose here that the coordination of the nitrogen atom to the Zn metal center increases the acidity and hydrogen-bonding capabilities of its hydrogen atoms. The energy inclination for the **1a**·Zn_2@(*R*,*R*-**2**)$_2$-(+) diastereoisomer is in complete agreement with the observed inversion of chirality. The CD spectra calculated for both diastereoisomeric complexes are depicted in Figure 11. The energetic stabilization of the *in-in* conformer is expected to increase with stronger intramolecular hydrogen-bonding interactions. We speculate that the higher amplitude observed in the CD of the 1:2 complex registered in TOL solution compared to DCM is a direct consequence of the formation of stronger intramolecular hydrogen bonds in the less-polar solvent (TOL).

The 1:2 complex could also adopt the *out-out* conformation (Figure 12). Optimization of this conformer leads to a C_2 symmetric structure, showing the formation of hydrogen bonding between the NHs of the free amine and the carbonyl oxygen atoms of the amide groups of the spacer. Because of the unfavorable characteristics of amines as hydrogen-bond donors, the formed hydrogen bonds should be very weak. Nevertheless, the calculations assign a lower energy to the *out-out* conformer of the **1a**·Zn_2@(*R*,*R*-**2**)$_2$ complex compared with that of the *in-in* analogues. Although the formation in solution of the *out-out* conformer cannot be ruled out, its structure does not support the blue shift observed in the Soret band of the UV−vis spectrum of the 1:2 complex. Additionally, the predicted CD spectrum for the *out-out* conformer does not agree with that observed experimentally. A plausible scenario is the formation of the 2:1 complex as a mixture of conformers involved in fast chemical equilibria, and the *in-in* conformer with a positive twist between the effective transition dipole moments of the porphyrin units being the major contributor to the experimentally observed CD spectrum.

dx.doi.org/10.1021/ic202515v | *Inorg. Chem.* 2012, 51, 4620−4635

Supramolecular Chirality Induction in the Coordination of Bisporphyrin Tweezer 1·Rh$_2$ with Enantiopure Ligand 2. We commented above that the value of the microscopic binding constant for the interaction R-NH$_2$···Rh-(III)-I is too high to be measured accurately even using absorption spectroscopy. This is also the case for the stability constants of the 1:1 and 1:2 complexes if they were produced in separated phases of the chirogenesis process of **1**·Rh$_2$ induced by coordination with **2**. We performed the spectroscopic titrations of bisporphyrin **1**·Rh$_2$ in TOL and DCM solutions with diamine *R,R*-**2** using the same methodology described for **1**·Zn$_2$. We observed that the maximum of the absorption Soret band of free **1**·Rh$_2$ in TOL solution is centered at λ = 414 nm. The initial addition of *R,R*-**2**, induces a decrease in the intensity of the Soret absorption and the appearance of a new absorption band at 425 nm. We assign this 11 nm shift of the Soret band to the formation of a 1:1 complex, **1**·Rh$_2$⊃*R,R*-**2**, in which the porphyrin binding sites are excitonically coupled. During the initial phase of the titration, a sharp isosbestic point was detected, suggesting that the formation of the 1:1 complex is the main process. Upon addition of more *R,R*-**2**, the titration entered a nonisosbestic phase. This is a result of the simultaneous existence of two binding events: the formation of the 1:1 complex and its destruction to afford the 1:2 complex. In the last stages, the titration entered another isosbestic phase since the only process taking place is the formation of the 1:2 complex from the 1:1. During the last phase, the band at 425 nm shifted to 430 nm. As observed for the reference system **5**·Rh/**7** in TOL, a Soret absorption at 435 nm is typical for a 1:1 complex of an axially coordinated monoamine to a Rh(III) porphyrin. It is probable that the 5 nm blue shift observed for the final Soret band is due to the existence of residual exciton coupling between the porphyrin units of the 1:2 complex, similar to the case explained above for bisporphyrin **1**·Zn$_2$. The complexation process of *R,R*-**2** with **1**·Rh$_2$ was also monitored using NMR spectroscopy in TOL solution. The incremental addition of up to 1 equiv of amine produces the appearance of proton signals in the upfield region (0 to −8 ppm) of the ^{1}H NMR spectra (Figure 13). The number of signals and their chemical shifts are almost coincident with the ones observed for the titration of **5**·Rh with *R,R*-**2** up to the addition of 0.5 equiv of diamine (Figure 6). These signals correspond to the protons of *R,R*-**2** sandwiched between two porphyrin units, and the similarity of spectra hints to an analogy of the sandwich complexes' structures. In the case of **5**·Rh, the addition of more than 0.5 equiv of *R,R*-**2** induced the destruction of the 2:1 intermolecular sandwich complex (**5**·Rh)$_2$⊃*R,R*-**2** and produced the appearance of a new set of proton signals corresponding to the 1:1 complex **5**·Rh@*R,R*-**2**. In contrast, for bisporphyrin **1**·Rh$_2$, the sandwich complex formed with *R,R*-**2**, **1**·Rh$_2$⊃*R,R*-**2** has a 1:1 stoichiometry and is intramolecular (see the Supporting Information for additional characterization). In the presence of more than 1 equiv of *R,R*-**2**, the 1:1 sandwich complex opens up to form a 1:2 complex **1**·Rh$_2$@(*R,R*-**2**)$_2$. The high number of signals observed for the protons of the coordinated diamine in the **1**·Rh$_2$@(*R,R*-**2**)$_2$ complex is probably due to both the slow rotation on the NMR time scale of the C_{meso}−$C_{amidophenyl}$ bonds and the desymmetrization of the bound ligand.

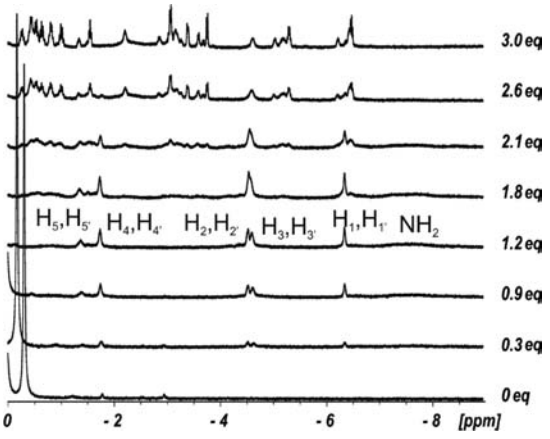

Figure 13. Upfield region of the ^{1}H NMR spectra registered during the titration of bisporphyrin **1**·Rh$_2$ with *R,R*-**2** in TOL solution. The fact that the 1:1 sandwich complex opens up in the presence of more than 1 equiv of diamine is indicative of a low EM value (vide infra).

First, we attempted the mathematical analysis of the UV−vis titration data of **1**·Rh$_2$ with *R,R*-**2** in TOL solution using the Specfit software.[53] We fixed the stability constants of the two complexes, 1:1 and 1:2, to their statistically estimated values using the following equations, $K_{1:1} = 2\alpha_P\alpha_L K_m^2$EM and $K_{1:2} = 4\alpha_P K_m^2$. We applied the values of K_m and cooperativity factors ($\alpha_P\alpha_L$) derived from the study of the model systems. We had used a similar strategy for the successful fitting of the titration data of **1**·Rh$_2$ with **7** in the study of model systems. In the case at hand, we also considered that the EM value calculated for the systems **1**·Zn$_2$/*R,R*-**2** was applicable to the **1**·Rh$_2$ analogue. Surprisingly to us, this procedure led to unacceptable fits of the experimental UV−vis titration data to the theoretical binding isotherms.

Next, the fit of the UV−vis titration data in TOL was assayed by fixing the spectrum of free bisporphyrin **1**·Rh$_2$ and $K_{1:2}$ to the statistically estimated lower value, as indicated above. With this procedure, the spectral signatures calculated for the UV−vis spectra of the two complexes, 1:1 and 1:2, were in full agreement with their expected binding geometries. The calculated absorption spectra displayed absorption maxima at 425 and 430 nm, for the **1**·Rh$_2$⊃*R,R*-**2** and **1**·Rh$_2$@(*R,R*-**2**)$_2$ species, respectively. Moreover, the good fit obtained for the titration data to the theoretical binding isotherms at different wavelengths provided an indication of the quality of this data analysis. The optimized value of $K_{1:1}$ returned from the fitting was 5.0 ± 1.0 × 10^9 M^{-1}, close to 3 orders of magnitude smaller than the value statistically estimated as the lower limit (1.5 × 10^{12} M^{-1}).

The absolute value of $K_{1:1}$ is clearly too high to be determined accurately from the fit of the titration data corresponding to its formation (initial phase of the titration). However, since the formation and destruction of the 1:1 complex occurs simultaneously in the middle phase of the titration, the mathematical analysis of the titration data described above allowed the precise determination of the ratio $K_{1:2}/K_{1:1}$ independently of the K_m value used, as long as it is considered to be equal or higher than the lower estimate 10^8 M^{-1}.[42] The equilibrium constant for the destruction process of the 1:1 complex to afford the 2:1 corresponds to the ratio of stability constants of the complexes $K_{1:1\leftrightarrow1:2} = K_{1:2}/K_{1:1}$. In short, fixing $K_{1:2}$ to a statistical estimate, the fitting procedure allows for a satisfactory evaluation of the magnitude of $K_{1:1}$ in relationship to the estimated $K_{1:2}$. Sound values for the EM operative in the 1:1 complex can subsequently be calculated from $K_{1:1}$ or, alternatively, $K_{1:1\leftrightarrow1:2}$.

dx.doi.org/10.1021/ic202515v | Inorg. Chem. 2012, 51, 4620−4635

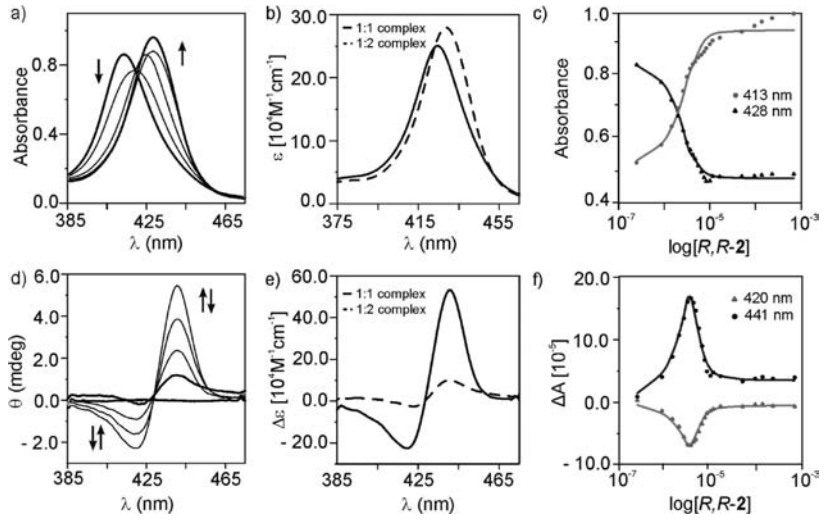

Figure 14. (a) UV−vis and (d) CD spectra obtained during the titration of **1**·Rh_2 and *R,R*-**2** in toluene solution at 298 K. The curves correspond to the addition of 0, 0.4, 1.1, 2.2, and 28.1 equiv of *R,R*-**2**. Calculated spectra for the 1:1 (continuous line) and 1:2 complexes (dashed line): (b) UV−vis (Soret band) and (e) CD. Fit of the titration data to the theoretical binding isotherm at selected wavelengths: (c) UV−vis and (f) CD.

Table 3. Calculated Stability Constants Values, $K_{1:1}$ and $K_{1:2}$, for the *R,R*-2/1·Zn_2 System. Calculated Stability Constants $K_{1:1}$ and Statistically Estimated $K_{1:2}$ Values for *R,R*-2/1·Rh_2. Measured Spectral UV−vis Characteristics of Free Bisporphyrins and Calculated Values for the Two Complexes in Which They Are Involved Are Represented

	free	1:1 complex		1:2 complex	
solvent, porphyrin	λ_{max}, fwhm[a], ε [nm, nm, 10^5 M^{-1} cm^{-1}]	$K_{1:1}$ [M^{-1}]	λ_{max}, fwhm[a], ε [nm, nm, 10^5 M^{-1} cm^{-1}]	$K_{1:2}$ [M^{-2}]	λ_{max}, fwhm[a], ε [nm, nm, 10^5 M^{-1} cm^{-1}]
TOL, **1**·Zn_2	423, 14, 8.4	$6.7 \pm 1.3 \times 10^4$	424, 9, 9.5	$4.5 \pm 0.9 \times 10^9$	426, 12, 8.8
DCM, **1**·Zn_2	421, 15, 9.8	$1.0 \pm 0.2 \times 10^6$	423, 11, 9.4	$7.9 \pm 1.6 \times 10^9$	429, 15, 8.3
TOL, **1**·Rh_2	414, 31, 2.5	$5.0 \pm 1.0 \times 10^9$	424, 30, 2.5	1.0×10^{16}[b]	429, 28, 2.8
DCM, **1**·Rh_2	418, 35, 3.4	$2.9 \pm 0.6 \times 10^{11}$	424, 29, 3.8	4.0×10^{17}[b]	431, 27, 4.6

[a]fwhm: full width at half-maximum. [b]Statistical estimates $K_{1:2} = 2\alpha_p K_m^2$.

We then probed the supramolecular chirogenesis of the **1**·Rh_2/*R,R*-**2** system also in TOL solution using CD spectroscopy. The incremental addition of *R,R*-**2** to a TOL solution of **1**·Rh_2, maintained at a constant concentration, initially produced the appearance and stepwise increase of a positive CD couplet, followed by a decrease in its amplitude. The multivariate analysis of the CD data titration fixing $K_{1:2}$ to the statistically calculated value and K_{11} to the calculated value from the UV titration provided a good fit and returned the spectral parameters for the observed chirality induction processes. Both **1**·Rh_2⊃*R,R*-**2** and **1**·Rh_2@(*R,R*-**2**)$_2$ complexes were assigned with positive couplets. As could be expected, the amplitude of the 1:1 complex **1**·Rh_2⊃*R,R*-**2** is higher (6-fold) than that of the 2:1 complex **1**·Rh_2@(*R,R*-**2**)$_2$. This result shows that the bisporphyrin **1**·Rh_2 does not express stoichiometrically controlled chirality inversion. It is worth noting that the sign of the couplet associated with the 1:1 complex **1**·Rh_2⊃*R,R*-**2** (positive) is opposite with respect to that of the couplet (negative) displayed by the analogous **1**·Zn_2⊃*R,R*-**2** complex. The changes observed in the CD spectra are associated with the initial formation of the 1:1 complex, followed by its destruction in the presence of more than 1 equiv of *R,R*-**2**, to afford the 1:2 complex.

Similar titrations were performed with the same **1**·Rh_2/*R,R*-**2** system in DCM solution. The value of $K_{1:2}$ was again statistically calculated with the same equation described above, but taking into account a 5-fold increase in the K_m value when moving from TOL to DCM and α_p = 0.8 (see the model systems). Fixing $K_{1:2} = 3.7 \times 10^{17}$ M^{-2} and the spectrum of free bisporphyrin, we obtained a good fit of the UV titration data to the theoretical binding isotherm, which gives some support to the quality of the data analysis. The returned value of $K_{1:1}$ was 2.9×10^{11} M^{-1}, again 3 orders of magnitude smaller than the statistical estimate (1.1×10^{14} M^{-1}). The calculated absorption spectra for **1**·Rh_2⊃*R,R*-**2** and **1**·Rh_2@(*R,R*-**2**)$_2$ returned from the fit displayed absorption maxima at 425 and 435 nm, respectively. The 10 nm blue shift of the Soret band assigned to the **1**·Rh_2⊃*R,R*-**2** with respect to **1**·Rh_2@(*R,R*-**2**)$_2$ supported the existence of exciton coupling in the 1:1 complex (Figure 14). On the contrary, the coincidence in absorption maxima for **1**·Rh_2@(*R,R*-**2**)$_2$ and the model system **7**@**5**·Rh indicates the lack of exciton in the 1:2 aggregate. The multivariate factor analysis of the CD titration data in DCM, using the same methodology described for the analysis in TOL solution, assigned a positive couplet to the 1:1 complex **1**·Rh_2⊃*R,R*-**2** and a silent CD to **1**·Rh_2@(*R,R*-**2**)$_2$. The amplitudes of the positive couplets assigned to the **1**·Rh_2⊃*R,R*-**2**, 1:1 complex, in TOL and DCM, are of the same order (1×10^2). A silent CD for the 2:1 complex, **1**·Rh_2@(*R,R*-**2**)$_2$, in DCM agrees with the lack of exciton coupling we assigned to the high stoichiometry complex in this solvent. This result is also in full agreement with our hypothesis stating that the amount of the 1:2 complex that adopts the *in-in* conformer is higher in TOL than in DCM. The intramolecular hydrogen bonding that stabilizes the *in-in* conformer is more favorable in the less-polar TOL solvent.

Table 3 lists the stability constant values $K_{1:1}$ and $K_{1:2}$ calculated for the system *R,R*-**2**/**1**·Zn_2 from the fit of the UV−vis

dx.doi.org/10.1021/ic202515v | *Inorg. Chem.* 2012, 51, 4620−4635

Table 4. Determined CD Spectral Data (CD Sign, Peak Position/nm, *A* Total Amplitude/M^{-1} cm^{-1}) of the Complexes (1:1 and 1:2) of Bisporphyrins **1**·Zn_2 and **1**·Rh_2 upon Coordination with *R,R*-**2**

		1:1 complex			1:2 complex		
solvent	porphyrin	FC[a]	SC[b]	A[c] [M^{-1} cm^{-1}]	FC[a]	SC[b]	A[c] [M^{-1} cm^{-1}]
TOL	**1**·Zn_2	−439	425	757	441	−427	420
DCM	**1**·Zn_2	−438	423	620	441	−426	150
TOL	**1**·Rh_2	441	−420	79	441	−423	17
DCM	**1**·Rh_2	438	−418	102	[d]	[d]	[d]

[a]FC: first Cotton effect. [b]SC: second Cotton effect. [c]*A*: total amplitude; $A = |\Delta\varepsilon_1 - \Delta\varepsilon_2|$. [d]As the CD signal was too small to be significant, a silent CD was assigned in the fitting.

titration data to a theoretical binding model considering three colored stoichiometric states of the porphyrin (free, 1:1 and 1:2 complexes). Calculated $K_{1:1}$ and estimated $K_{1:2}$ values for the system *R,R*-**2**/**1**·Rh_2 are also listed in the table. Table 4 summarizes the CD spectral parameters of the two complexes returned from the data fitting of the CD titrations fixing the stability constant values too those obtained from the UV−vis titrations.

Several examples of related Zn-porphyrin tweezer receptors binding enantiopure diamine **2** have been described in the literature.[19,11,20,43,44] The stability constant values determined for the **1**·Zn_2⊃*R,R*-**2** are in complete agreement with the magnitudes reported for related sandwich complexes (10^5−10^7 M^{-1}). Only in two of the previous reports,[19,20] however, the stability constants of the open 1:2 complexes are indicated and again we observed a complete coincidence with the values presented here (10^9−10^{10} M^{-2}). The spectral changes (CD and UV−vis) observed in the titration experiments of **1**·Zn_2 and *R,R*-**2** show very good correlation with those described for the interaction of the analogous bifunctional diamine *R,R*-1,2-diphenylethylenediamine (DPEA) and the ethane-bridged bis-Zn-octaethylporphyrin.[20] DPEA exhibited the unique property of both chirality induction and inversion. Analogously, diamine *R,R*-**2** turned out to be an appropriate ditopic ligand for controlling supramolecular chirality induction and inversion in achiral **1**·Zn_2. The process is also occurring via a consecutive two-step binding mechanism involving the formation of two complexes with 1:1 and 1:2 (bisporphyrin−amine) stoichiometry.

The *A* values of 757 and 620 M^{-1} cm^{-1} calculated for the **1**·Zn_2⊃*R,R*-**2** in TOL and DCM solutions, respectively, are extremely high. To the best of our knowledge, these are one of the largest values reported for the chirality induction process involving achiral Zn-bisporphyrin receptors and *R,R*-**2**. Ema et al. reported an *A* value of approximately 500 M^{-1} cm^{-1} in the interaction of *R,R*-**2** and a chiral Zn-bisporphyrin.[42] The remarkable high values of *A* for the **1**·Zn_2⊃*R,R*-**2** complex are due to optimal geometry factors, that is, intertransition distance and angle. We have not found reported *A* values for the open 1:2 complexes resulting from the interaction of Zn-bisporphyrins with ditopic amines, although we can deduce from the figures shown in the reports that they should be considerable smaller than those assigned to the sandwich 1:1 complexes. In this regard, Borovkov et al. described *A* values for several 1:2 complexes of the bis-Zn-octaethylporphyrin with monotopic chiral amines on the order of 10^2 M^{-1} cm^{-1}.[45] This value is in line with the calculated *A* for the **1**·Zn_2@(*R,R*-**2**)$_2$ complex formed in DCM solution. In striking contrast, the *A* value for the same complex in TOL solutions increases to 420 M^{-1} cm^{-1}. It is worth to note that monotopic chiral amines, such as *S*-**8**, did not induce the formation of a CD-active 1:2 complex with **1**·Zn_2. As discussed above, we deduced that the ditopic nature of the ligand is fundamental to yield CD activity in the 1:2 complexes of **1**·Zn_2.

The stability constants reported here for the 1:1 and 1:2 complexes of *R,R*-**2** with **1**·Rh_2 in TOL and DCM solutions should be considered as lower limit estimates. As far as we are aware, there are no reports of the accurate thermodynamic characterization of iodo-Rh(III)-bisporphyrin complexes with amines due to their high thermodynamic stability. It is known, however, that Rh(III)-alkyl porphyrins having a trans organic ligand, that is, methyl in place of the halogen, show a significant reduction of binding affinity toward amines (K_a values on the order of 10^5 M^{-1}).[46,22] The UV−vis absorption spectra of **1**·Rh_2 compares well with the electronic absorption data reported for the parent **5**·Rh monoporphyrin lacking the *p*-pentyl substituents.[47] The spectral signatures of the 1:1 and 1:2 complexes of *R,R*-**2** with **1**·Rh_2 are in line with those observed for the analogous complexes with **1**·Zn_2. The coordination of the amine ligand induces a red shift in the Soret band of **1**·Rh_2, similar to what have been reported for the coordination with P, S, and Se ligands.[48,49] This study constitutes the first report of supramolecular chirality induction using achiral iodo-Rh(III)-bisporphyrin and ditopic enantiopure amine. Most likely, the decrease in the calculated *A* values for the 1:1 and 1:2 complexes of **1**·Rh_2 compared with **1**·Zn_2 is related to the 3-fold diminution of the exciton coefficient of the former. The couplet amplitude is proportional to the square of the extinction coefficient of the coupled chromophores.[5] However, changes in the geometrical parameters of the complexes (interchromophoric distance and angle) caused by the metal substitution cannot be ruled out.

As commented above, the calculated values for $K_{1:1\leftrightarrow1:2} = K_{1:2}/K_{1:1}$ corresponding to the destruction of the 1:1 sandwich complex **1**·Rh_2⊃*R,R*-**2** in TOL and DCM solutions are appropriate to determine the corresponding EM values.[42] We used the relationship $K_{1:1\leftrightarrow1:2} = 2/\alpha_L EM$, where $\alpha_L = 0.03$, we determined EM values of $3.3 \pm 1.6 \times 10^{-5}$ and $4.8 \pm 2.4 \times 10^{-5}$ M in TOL and DCM, respectively. Interestingly, the values of EMs determined for the N···Rh(III)-I intramolecular interaction in the **1**·Rh_2⊃*R,R*-**2** complex are 3 orders of magnitude smaller that the corresponding values for the N···Zn(II) interaction embedded in the analogous scaffolding complex **1**·Zn_2⊃*R,R*-**2**. This observation suggests the existence of interplay between the strength of K_m and EM. Since EM is expected to decrease with restriction of conformational flexibility and conformational strain, we hypothesize that the much stronger N···Rh(III)-I intermolecular interaction is responsible for the observed reduction in EM values. The complex **1**·Rh_2⊃*R,R*-**2** is vibrationally more restricted than **1**·Zn_2⊃*R,R*-**2**. A more far-reaching implication of our finding has to do with the fact that EM values cannot be considered as

dx.doi.org/10.1021/ic202515v | *Inorg. Chem.* 2012, 51, 4620−4635

independent properties of supramolecular scaffolds. EM values seem to be modulated by the strength of the interaction. This is also the basis to explain the unacceptable fit of the titration UV−vis data we obtained in the **1**·Rh_2/*R*,*R*-**2** system using statistically estimated values of $K_{1:1}$ based on the EM value determined for the **1**·Zn_2/*R*,*R*-**2** system. The existence of interplay between K_m and EM has been postulated previously by Hunter et al. using zinc porphyrin−pyridine complexes that contain additional intramolecular H-bonding interactions.[50,51]

The investigation of the structural and electronic factors that control the observed changes in the induction of chirality for the **1**·Rh_2 system compared to the Zn(II) analogue proved to be difficult due to associated complexity in DFT calculations of the former. Assuming that the 1:1 complexes **1**·Rh_2⊃*R*,*R*-**2** and **1**·Zn_2⊃*R*,*R*-**2** can adopt similar structures, the change in sign of their associated couplet must be related to the change in the sense of the twist between the "privileged" transition dipole moments of the porphyrin units. On the basis of the chirality exciton theory, the sense of the twist is anticlockwise in the more stable diastereoisomer of **1**·Zn_2⊃*R*,*R*-**2** and should be clockwise for the lower-energy diastereoisomer of **1**·Rh_2⊃*R*,*R*-**2**. A change in the relative distribution of the two chiral sandwich 1:1 diastereoisomeric complexes **1**·M_2⊃*R*,*R*-**2**-(-) and **1**·M_2⊃*R*,*R*-**2**-(+) as a function of the metal center, Zn or Rh, is not unexpected because of the small difference in energy computed for the two Zn analogues.

CONCLUSIONS AND GENERAL COMMENTS

The CD activity observed for the 1:1 and 1:2 complexes of bisporphyrins **1**·M_2 upon binding *R*,*R*-**2** is due to the existence of energetically more favored structures (stereodifferentiation) having an asymmetric twist between the "privileged" transition dipole moments associated with the porphyrin units and to the existence of exciton coupling between them. A shorter distance and an energetically preferred cofacial arrangement of the porphyrin units and the interacting dipole moments are common to the structures of the 1:1 complexes, resulting in associated CD spectra displaying bisignate Cotton effects (couplets) of large amplitude. Unexpectedly, some 1:2 (bisporphyrin/diamine) complexes are also associated with CD spectra showing a bisignate Cotton effect but having much smaller amplitudes. This observation suggests that, in the 1:2 complexes, the distance between chromophores is larger and their relative arrangement is probably less defined (more conformers of similar energies are possible).

A sensitive reduction in the amplitude values of the couplets corresponding to the supramolecular complexes of **1**·Rh_2/*R*,*R*-**2** compared to those of **1**·Zn_2/*R*,*R*-**2** is observed. Because the couplet amplitude is proportional to the square of extinction coefficients of the coupled chromophores, the reduction in extinction coefficients of Rh(III) porphyrin compared to Zn(II) counterparts is responsible for the observed amplitude diminution. On the other hand, **1**·Rh_2 bisporphyrin produces complexes with *R*,*R*-**2** that are more kinetically and thermodynamically stable than **1**·Zn_2. The most important effects of the modification of the metal center in the chirogenesis process are (a) the change in sign of the bisignate Cotton effect assigned to the 1:1 complexes and (b) the lack of chirality inversion for the 1:2 complex of the **1**·Rh_2 bisporphyrin. The change in the solvent used to probe the chirogenesis process (TOL or DCM) has subtle effects in the kinetic and thermodynamic stability of the complexes. Likewise, the amplitudes of the couplets for the 1:1 complexes are not sensitive to solvent change. On the contrary, the chiral activity of the 1:2 complexes is highly solvent-dependent. TOL favors the formation of 1:2 complexes with higher amplitude values. Most likely, this is due to a favorable cofacial-like arrangement (conformational preference) of the porphyrin units in the 1:2 complexes formed in TOL solution. We speculate on the possible formation of intramolecular hydrogen bonds between the amino groups of the ligands involved in the 1:2 complex. These interactions will be fundamental in fixing the relative spatial orientation and distance of the chromophores attained in the *in-in* conformation of the complex. Our hypothesis is substantiated by the observation of silent CDs for the 1:1 and 1:2 complexes derived from **1**·M_2 and monotopic chiral amines. Amines are not very good hydrogen-bond donors, but reasonably good hydrogen-bond acceptors through the basic nitrogen atom. We assume that the coordination of the metal (Rh or Zn) to the nitrogen atom should increase the Lewis and Brönsted acidity of the attached hydrogen atoms and their hydrogen-bond donor capabilities. The hydrogen-bonding interactions are expected to be maximized in TOL due to its reduced dielectric constant, dipole moment, and hydrogen-bonding capabilities compared to those of DCM. In fact, it has specifically been shown that the interaction of DCM with polar groups (methyl esters) renders the chirality induction mechanism solvent-dependent.[52] Interestingly, the values of EM for the N···Rh(III)-I intramolecular interaction in the **1**·Rh_2⊃*R*,*R*-**2** complex are 3 orders of magnitude smaller than the corresponding values for the N···Zn(II) interaction embedded in the analogous scaffold of **1**·Zn_2⊃*R*,*R*-**2**. This observation suggests the existence of interplay between the strength of K_m and EM. Contrary to current dogmas, our results indicate that the EM value cannot be considered an independent property of supramolecular scaffolds. EM values are modulated by the strength of the intermolecular interaction (K_m) used in the assembly process. In turn, for the system under study, K_m values are strongly metal-dependent but show weak solvent effects.

ASSOCIATED CONTENT

Supporting Information

Computational details; *xyz* coordinates for all minimized structures; experimental procedures for the synthesis of bisporphyrins **1**·M_2 and related characterization data; 2D spectra of the **1**·M_2, their sandwich complexes, and *R*,*R*-**2**; general procedure employed in the spectroscopic titrations; binding equilibria for the model systems; mathematical analyses of the obtained titration data; and the X-ray crystallographic file (CIF) for **5**·Rh·MeOH. This material is available free of charge via the Internet at http://pubs.acs.org.

AUTHOR INFORMATION

Corresponding Author

*E-mail: pballester@iciq.es (P.B.).

Notes

The authors declare no competing financial interest.

ACKNOWLEDGMENTS

We thank Spanish Ministerio de Economía y Competitividad (CTQ2011-23014 and CTQ2011-29054-C02-02), Generalitat de Catalunya (2009SGR00462, 2009SGR00686), and ICIQ Foundation for funding.

REFERENCES

(1) Berova, N., Nakanishi, K., Woody, R. W., Eds. *Circular Dichroism: Principles and Applications*; John Wiley: New York, 2000.
(2) Huang, X.; Nakanishi, K.; Berova, N. *Chirality* **2000**, *12*, 237−255.
(3) Matile, S.; Berova, N.; Nakanishi, K.; Novkova, S.; Philipova, I.; Blagoev, B. *J. Am. Chem. Soc.* **1995**, *117*, 7021−7022.
(4) Harada, N.; Chen, S. L.; Nakanishi, K. *J. Am. Chem. Soc.* **1975**, *97*, 5345−5352.
(5) Heyn, M. P. *J. Phys. Chem.* **1975**, *79*, 2424−2426.
(6) Matile, S.; Berova, N.; Nakanishi, K.; Fleischhauer, J.; Woody, R. W. *J. Am. Chem. Soc.* **1996**, *118*, 5198−5206.
(7) Ercolani, G. *J. Am. Chem. Soc.* **2003**, *125*, 16097−16103.
(8) Ercolani, G.; Schiaffino, L. *Angew. Chem., Int. Ed.* **2011**, *50*, 1762−1768.
(9) Hunter, C. A.; Anderson, H. L. *Angew. Chem., Int. Ed.* **2009**, *48*, 7488−7499.
(10) Whitty, A. *Nat. Chem. Biol.* **2008**, *4*, 435−439.
(11) Borovkov, V. V.; Fujii, I.; Muranaka, A.; Hembury, G. A.; Tanaka, T.; Ceulemans, A.; Kobayashi, N.; Inoue, Y. *Angew. Chem., Int. Ed.* **2004**, *43*, 5481−5485.
(12) Grimme, S.; Siering, C.; Torang, J.; Kruse, H.; Waldvogel, S. R. *Chem. Commun. (Cambridge, U.K.)* **2010**, *46*, 1625−1627.
(13) Borovkov, V. V.; Bhyrappa, P.; Inoue, Y. *Org. Lett.* **2007**, *9*, 433−435.
(14) Beletskaya, I.; Tyurin, V. S.; Tsivadze, A. Y.; Guilard, R.; Stern, C. *Chem. Rev. (Washington, DC, U.S.)* **2009**, *109*, 1659−1713.
(15) Berova, N.; Di Bari, L.; Pescitelli, G. *Chem. Soc. Rev.* **2007**, *36*, 914−931.
(16) Hembury, G. A.; Borovkov, V. V.; Inoue, Y. *Chem. Rev. (Washington, DC, U.S.)* **2007**, *108*, 1−73.
(17) Berova, N.; Pescitelli, G.; Petrovic, A. G.; Proni, G. *Chem. Commun. (Cambridge, U.K.)* **2009**, 5958−5980.
(18) Borovkov, V. V.; Inoue, Y. *Top. Curr. Chem.* **2006**, *265*, 89−146.
(19) Etxebarria, J.; Vidal-Ferran, A.; Ballester, P. *Chem. Commun. (Cambridge, U.K.)* **2008**, 5939−5941.
(20) Borovkov, V. V.; Lintuluoto, J. M.; Inoue, Y. *Org. Lett.* **2002**, *4*, 169−171.
(21) Aoyama, Y.; Asakawa, M.; Yamagishi, A.; Toi, H.; Ogoshi, H. *J. Am. Chem. Soc.* **1990**, *112*, 3145−3151.
(22) Kim, H. J.; Redman, J. E.; Nakash, M.; Feeder, N.; Teat, S. J.; Sanders, J. K. M. *Inorg. Chem.* **1999**, *38*, 5178−5183.
(23) Redman, J. E.; Feeder, N.; Teat, S. J.; Sanders, J. K. M. *Inorg. Chem.* **2001**, *40*, 2486−2499.
(24) Fukushima, K.; Funatsu, K.; Ichimura, A.; Sasaki, Y.; Suzuki, M.; Fujihara, T.; Tsuge, K.; Imamura, T. *Inorg. Chem.* **2003**, *42*, 3187−3193.
(25) Redman, J. E. Ph.D. dissertation, University of Cambridge, Cambridge, UK, 2000.
(26) Tsutsumi, O.; Sato, H.; Takeda, K.; Ogawa, T. *Thin Solid Films* **2006**, *499*, 219−223.
(27) Bond, A. D.; Sanders, J. K. M.; Stulz, E. *New J. Chem.* **2011**, *35*, 2691−2696.
(28) Aoyama, Y.; Nonaka, S.; Motomura, T.; Ogoshi, H. *Chem. Lett.* **1989**, 1877−1880.
(29) Aoyama, Y.; Yamagishi, A.; Asagawa, M.; Toi, H.; Ogoshi, H. *J. Am. Chem. Soc.* **1988**, *110*, 4076−4077.
(30) Simonato, J. P.; Pecaut, J.; Marchon, J. C. *Inorg. Chim. Acta* **2001**, *315*, 240−244.
(31) Mullen, K. M.; Gunter, M. J. *J. Org. Chem.* **2008**, *73*, 3336−3350.
(32) Hunter, C. A.; Gardner, M.; Guerin, A. J.; Michelsen, U.; Rotger, C. *New J. Chem.* **1999**, *23*, 309−316.
(33) Planells, M.; Pelleja, L.; Ballester, P.; Palomares, E. *Energy Environ. Sci.* **2011**, *4*, 528−534.
(34) Forneli, A.; Planells, M.; Sarmentero, M. A.; Martinez-Ferrero, E.; O'Regan, B. C.; Ballester, P.; Palomares, E. *J. Mater. Chem.* **2008**, *18*, 1652−1658.
(35) Haino, T.; Fujii, T.; Fukazawa, Y. *J. Org. Chem.* **2006**, *71*, 2572−2580.
(36) Hunter, C. A.; Sarson, L. D. *Angew. Chem., Int. Ed. Engl.* **1994**, *33*, 2313−2316.
(37) The reported K_m value must be considered as a lower-limit estimate. UV−vis titrations carried out in toluene solution at the highest possible dilution (5×10^{-7} M) could not provide an accurate value of the binding constant. The shift of the Soret band reached saturation after the addition of just 1 equiv of amine. In a 1:1 THF/toluene mixture, a value of $K_m = 6 \times 10^7$ M^{-1} could be determined (Supporting Information). However, in neat THF or 1:1 THF/toluene solutions containing an excess of amine (more than 1 equiv), we detected the formation of a new species having two axially coordinated amines. In the more polar solvent, the substitution of the iodide in the 1:1 complex by a second equivalent of amine occurs and is facilitated by irradiation with UV light.
(38) Ballester, P.; Costa, A.; Castilla, A. M.; Deya, P. M.; Frontera, A.; Gomila, R. M.; Hunter, C. A. *Chem.—Eur. J.* **2005**, *11*, 2196−2206.
(39) Hunter, C. A.; Sanders, J. K. M.; Stone, A. J. *Chem. Phys.* **1989**, *133*, 395−404.
(40) Chekmeneva, E.; Hunter, C. A.; Packer, M. J.; Turega, S. M. *J. Am. Chem. Soc.* **2008**, *130*, 17718−17725.
(41) Pescitelli, G.; Gabriel, S.; Wang, Y. K.; Fleischhauer, J.; Woody, R. W.; Berova, N. *J. Am. Chem. Soc.* **2003**, *125*, 7613−7628.
(42) The fit of the titration data considering $K_m = 1 \times 10^{10}$ M^{-1} for the interaction N···Rh(III)-I afforded calculated EM values for the 1:1 complex identical to the ones obtained using $K_m = 1 \times 10^8$ M^{-1}.
(43) Ema, T.; Ouchi, N.; Doi, T.; Korenaga, T.; Sakai, T. *Org. Lett.* **2005**, *7*, 3985−3988.
(44) Borovkov, V. V.; Lintuluoto, J. M.; Sugiura, M.; Inoue, Y.; Kuroda, R. *J. Am. Chem. Soc.* **2002**, *124*, 11282−11283.
(45) Borovkov, V. V.; Lintuluoto, J. M.; Sugeta, H.; Fujiki, M.; Arakawa, R.; Inoue, Y. *J. Am. Chem. Soc.* **2002**, *124*, 2993−3006.
(46) Aoyama, Y.; Yamagishi, A.; Asagawa, M.; Toi, H.; Ogoshi, H. *J. Am. Chem. Soc.* **1988**, *110*, 4076−4077.
(47) Grass, V.; Lexa, D.; Momenteau, M.; Saveant, J. M. *J. Am. Chem. Soc.* **1997**, *119*, 3536−3542.
(48) Redman, J. E.; Feeder, N.; Teat, S. J.; Sanders, J. K. M. *Inorg. Chem.* **2001**, *40*, 3217−3221.
(49) Stulz, E.; Scott, S. M.; Bond, A. D.; Otto, S.; Sanders, J. K. M. *Inorg. Chem.* **2003**, *42*, 3086−3096.
(50) Hunter, C. A.; Misuraca, M. C.; Turega, S. M. *Chem. Sci.* **2012**, *3*, 589−601.
(51) Hunter, C. A.; Misuraca, M. C.; Turega, S. M. *J. Am. Chem. Soc.* **2011**, *133*, 582−594.
(52) Borovkov, V. V.; Hembury, G. A.; Inoue, Y. *Angew. Chem., Int. Ed.* **2003**, *42*, 5310−5314.
(53) (a) *SPECFIT*, version 3.0; Spectra Software Associates. (b) Gampp, H.; Maeder, M.; Meyer, C. J.; Zuberbühler, A. D. *Talanta* **1985**, *32*, 95−101. (c) Gampp, H.; Maeder, M.; Meyer, C. J.; Zuberbühler, A. D. *Talanta* **1986**, *33*, 943−351.